nature chemical biology



Article

https://doi.org/10.1038/s41589-025-01973-6

Directed evolution of LaccID for cell surface proximity labeling and electron microscopy

Received: 5 September 2024

Accepted: 6 June 2025

Published online: 1 August 2025



Song-Yi Lee **\textsup 1,2,3,16**, Heegwang Roh**, David Gonzalez-Perez **\textsup 5**, Mason R. Mackey**, Daniel Hoces **\textsup 1,8**, Colleen N. McLaughlin**, Chang Lin**, Stephen R. Adams**, Khanh Nguyen**, Keun-Young Kim**, David J. Luginbuhl**, Liqun Luo**, Namrata D. Udeshi **\textsup 1,**, Steven A. Carr **\textsup 1,**, Rogelio A. Hernández-López**, Mark H. Ellisman**, Miguel Alcalde **\textsup 5** & Alice Y. Ting **\textsup 1,4,12,13,14** \in \textsup 1,4,12,13,1

Enzymes that oxidize aromatic substrates have been harnessed for cell-based technologies including proximity labeling and electron microscopy; however, they are associated with drawbacks such as the need for toxic H_2O_2 . Here, we explore multicopper oxidases (laccases) as a new enzyme class for proximity labeling and electron microscopy in mammalian cells. LaccID was generated through 11 rounds of directed evolution from an ancestral fungal laccase and catalyzes one-electron oxidation of diverse aromatic substrates using O_2 instead of toxic H_2O_2 . Surprisingly, we found that LaccID is selectively active at the surface plasma membrane of both living and fixed cells. We use LaccID proximity labeling and mass spectrometry to map the changing surface proteome of T cells that engage with tumor cells through antigen-specific T cell receptors. In addition, we use LaccID as a genetically encodable tag for EM visualization of cell surface features in mammalian cell culture and in the fly brain. Our study paves the way for future cell-based applications of LaccID.

Proximity labeling has emerged as a powerful technique for mapping spatial proteomes, interactomes and transcriptomes in living cells and animals¹. Current proximity labeling enzymes fall largely into two classes: the peroxidases and the biotin ligases (Fig. 1a). Peroxidases such as APEX2 (ref. 2) and horseradish peroxidase (HRP)³ generate phenoxyl radicals from phenolic substrates and $\rm H_2O_2$, which subsequently react with surface-exposed electron-rich side chains such as tyrosines. These enzymes are fast and versatile, able to use a wide range of substrates, but

the requirement for H_2O_2 means that the labeling conditions are toxic, especially in tissue and animals. Labeling by biotin ligases, such as TurbolD⁴ and BiolD⁵, is milder; these enzymes use endogenous adenosine triphosphate (ATP) to generate biotinyl-5′-adenosine monophosphate, a mixed anhydride that reacts with lysine side chains. However, because these enzymes use biotin, it is difficult to avoid background from both endogenous biotin and endogenous biotinylated proteins ^{6,7}, which are abundant in vivo⁸. Furthermore, biotin ligases are generally not

¹Department of Genetics, Stanford University, Stanford, CA, USA. ²Department of New Biology, DGIST, Daegu, Republic of Korea. ³New Biology Research Center, DGIST, Daegu, Republic of Korea. ⁴Department of Chemistry, Stanford University, Stanford, CA, USA. ⁵Department of Biocatalysis, Institute of Catalysis, ICP-CSIC, Madrid, Spain. ⁶Department of Neurosciences, University of California, San Diego, La Jolla, CA, USA. ⁷Center for Research in Biological Systems and the National Center for Microscopy and Imaging Research, University of California, San Diego, La Jolla, CA, USA. ⁸Department of Bioengineering, Stanford University, Stanford, CA, USA. ⁹Department of Biology and Howard Hughes Medical Institute, Stanford University, Stanford, CA, USA. ¹⁰Department of Pharmacology, University of California, San Diego, La Jolla, CA, USA. ¹¹Broad Institute of MIT and Harvard, Cambridge, MA, USA. ¹²Chan Zuckerberg Biohub - San Francisco, San Francisco, CA, USA. ¹³Department of Biology, Stanford University, Stanford, CA, USA. ¹⁴The Phil & Penny Knight Initiative for Brain Resilience at the Wu Tsai Neurosciences Institute, Stanford, CA, USA. ¹⁵Present address: Howard Hughes Medical Institute, University of California, Berkeley, Berkeley, CA, USA. ¹⁶These authors contributed equally: Song-Yi Lee, Heegwang Roh. ⊠e-mail: ayting@stanford.edu

used for cell surface proteome mapping because ATP is absent in the extracellular environment. While ATP could be added exogenously, tissue penetration and unintentional activation of purine receptors are concerns. For these reasons, new proximity labeling enzymes that use different chemistries than existing enzymes are needed to advance the field.

Given the versatility of phenoxyl radicals for covalent tagging of proteins⁹, RNA¹⁰ and DNA¹¹ and for generating contrast for electron microscopy (EM)¹², we searched for APEX2-like oxidizing enzymes that do not require toxic H_2O_2 for labeling. Polyphenol oxidase (PPO) and laccase are both copper enzymes that oxidize phenol using O₂ instead of H₂O₂. Laccase drew our attention for several reasons. First, it catalyzes one-electron oxidation to generate short-lived phenoxyl radicals¹³. PPO, on the other hand, carries out two-electron oxidation to generate quinones¹⁴, which have much longer half-lives and, therefore, larger expected labeling radii. Second, laccase has a broad substrate scope, which includes diaminobenzidine (DAB)¹⁵, a reagent used to generate contrast for EM 12 . Third, the K_m value (Michaelis constant) of laccase for $O_2(20-50 \mu M)^{16}$ is in the range of physiological O_2 concentrations in tissue (29–64 μ M in the human brain for example ¹⁷), suggesting potential in vivo applicability. Fourth, laccase has been used for cell surface fluorescence imaging, albeit with antibody targeting rather than genetic encoding¹⁸. Lastly, fungal laccases¹⁹, which have a broader substrate scope and higher redox potential than their bacterial counterparts, have been engineered for numerous industrial applications, including paper-pulp biobleaching, textile dye decolorization, bioremediation, food processing and biofuel cells²⁰.

However, there are notable challenges to the use of laccases for proximity labeling technology, most importantly that no laccase has previously been expressed and shown to be active in mammalian cells. The enzyme is complex, with four copper atoms, two or more disulfides, glycosylation, optimal activity at acidic pH (pH 4–5) and an electron transfer pathway that is strongly interrupted by modest concentrations of hydroxyl anions or halides (for example, NaCl and KCl) in cell culture media²¹. Here, we benchmarked several engineered laccase templates^{22–25}, identified an ancestral fungal variant with slight activity in HEK293T cells and performed extensive directed evolution on the yeast surface to improve its activity (Fig. 1b). The resulting clone, LaccID, was deployed for both EM and cell surface proteome mapping in mammalian cells (Fig. 1a). Our work establishes a new enzyme class for proximity labeling with promising properties and paves the way for future improvements.

Results

Engineering LaccID

Laccases are widely expressed in fungi, plants, insects and bacteria¹³ but there is no mammalian counterpart. The natural function of laccases is to polymerize and depolymerize aromatic substrates involved in lignin degradation and biosynthesis, stress defense, pigment synthesis and sporulation²⁶. Laccases possess four copper atoms distributed into two copper centers. Fungal laccases also contain at least two disulfide bonds and are heavily glycosylated¹⁹. The most extensively engineered laccases for industrial applications are from white-rot fungi, which have been improved for activity in ionic liquids, high and low pH, high temperature and physiological fluids²⁶.

Given the lack of prior reports demonstrating laccase activity in mammalian systems, we first selected a panel of fungal laccase variants to test in HEK293T cells. We cloned them as fusions to a secretion signal, an epitope tag (V5) and transmembrane anchor (from CD4) for cell surface expression. Our panel consisted of (1) LacAnc100 (ref. 22), an ancestrally resurrected sequence from Basidiomycete PM1 fungi, which may offer improved heterologous expression and activity because of the generalist nature of ancient enzymes²⁷; (2) ChU-B²³, a mutant of PM1 laccase that was engineered for applications in human blood, withstanding neutral and alkaline pH and high halide concentrations;

(3) SCHEMA laccase²⁴, a chimeric laccase with improved stability engineered by SCHEMA–RASPP recombination; and (4) KyLO²⁵, a laccase mutant from ascomycetous *Myceliophthora thermophila* engineered for enhanced activity at pH 8.0.

All four laccases expressed well in HEK293T cells, as determined by anti-V5 western blotting (Fig. 1c). However, only a single laccase, LacAnc100, showed labeling activity when incubated with biotinphenol (BP) probe for 1 h. LacAnc100 exhibited a small degree of self-labeling (asterisk in Fig. 1c), which was less than the intensity of endogenous biotinylated protein bands and far lower than the promiscuous labeling catalyzed by HRP with BP and $\rm H_2O_2$ in just 1 min. However, this small activity provides a basis to carry out directed evolution of LacAnc100 to improve its properties.

We used yeast surface display for directed evolution (Fig. 1d) because of our past success with this platform for engineering APEX2 (ref. 2) and TurbolD 4 . In addition, fungal laccases have been functionally expressed in Saccharomyces cerevisiae at high titers 28 , indicating that yeast provide the necessary machinery for both copper insertion and glycosylation. We fused LacAnc100 to the yeast mating protein Aga2p for surface display and used error-prone PCR to create a library of variants with an average of 1–7 amino acid changes per gene.

BP labeling of the yeast library was followed by streptavidin-fluorophore staining and fluorescence-activated cell sorting (FACS) to enrich populations with high activity. Several strategies were used over 11 rounds of selection. First, we progressively increased selection stringency by reducing labeling time (Fig. 1e and Supplementary Figs. 1a, 2a and 3a). Second, at the end of each generation, all unique sequences were tested in HEK293T cells and beneficial mutations were manually combined (Supplementary Figs. 1–3) before diversification of the winning clone by error-prone PCR for further evolution. Third, in some rounds, half of the cell population was subjected to labeling in the presence of the radical quenchers sodium ascorbate and Trolox to reduce radical half-life and between-cell 'trans'-labeling; the populations were recombined after FACS enrichment (Supplementary Fig. 2).

In total, we performed 11 rounds of selection over three generations of evolution (Fig. 1e). FACS analysis of yeast showed a gradual increase in biotinylation efficiency over the course of evolution, with LaccID being fourfold more active than the original template LacAnc100 (Fig. 1f). This trend was reproduced when the clones were analyzed on the surface of HEK293T cells (Fig. 1g), with LaccID exhibiting both the highest expression and the highest activity-to-expression ratio of all clones.

LaccID optimization and characterization in mammalian cells

Although LaccID has higher biotinylation activity than the starting template LacAnc100, this activity is still much lower than that of HRP in a side-by-side comparison (Supplementary Fig. 4a). We hypothesized that the mammalian cell environment, including the culture medium, may impact LaccID activity. Thus, we tested different media compositions, comparing complete DMEM to RPMI and Earle's balanced salt solution (EBSS) (Fig. 2a). We found that labeling with BP was strongest in EBSS, perhaps because it lacks thiols that could inhibit laccase activity. In a separate test, we found that additives such as 10% FBS and 0.25 mM cysteine can impair LaccID activity in EBSS (Supplementary Fig. 4b).

We next hypothesized that substrate structure may influence biotinylation by LaccID. Many natural and synthetic substrates used by laccases have an *ortho*-methoxy substituent on the phenol, an electron-donating moiety that facilitates oxidation²⁹. When tested on LaccID-expressing HEK293T cells, biotin-methoxyphenol (BMP) showed higher labeling than BP (Fig. 2b) and comparable labeling in both RPMI and EBSS media (Supplementary Fig. 4c).

Substrate titration and time-course experiments showed that 1–2 h of labeling with 250–500 µM BP or BMP substrate provides an optimal signal-to-noise ratio (Supplementary Fig. 4d,e). Interestingly,

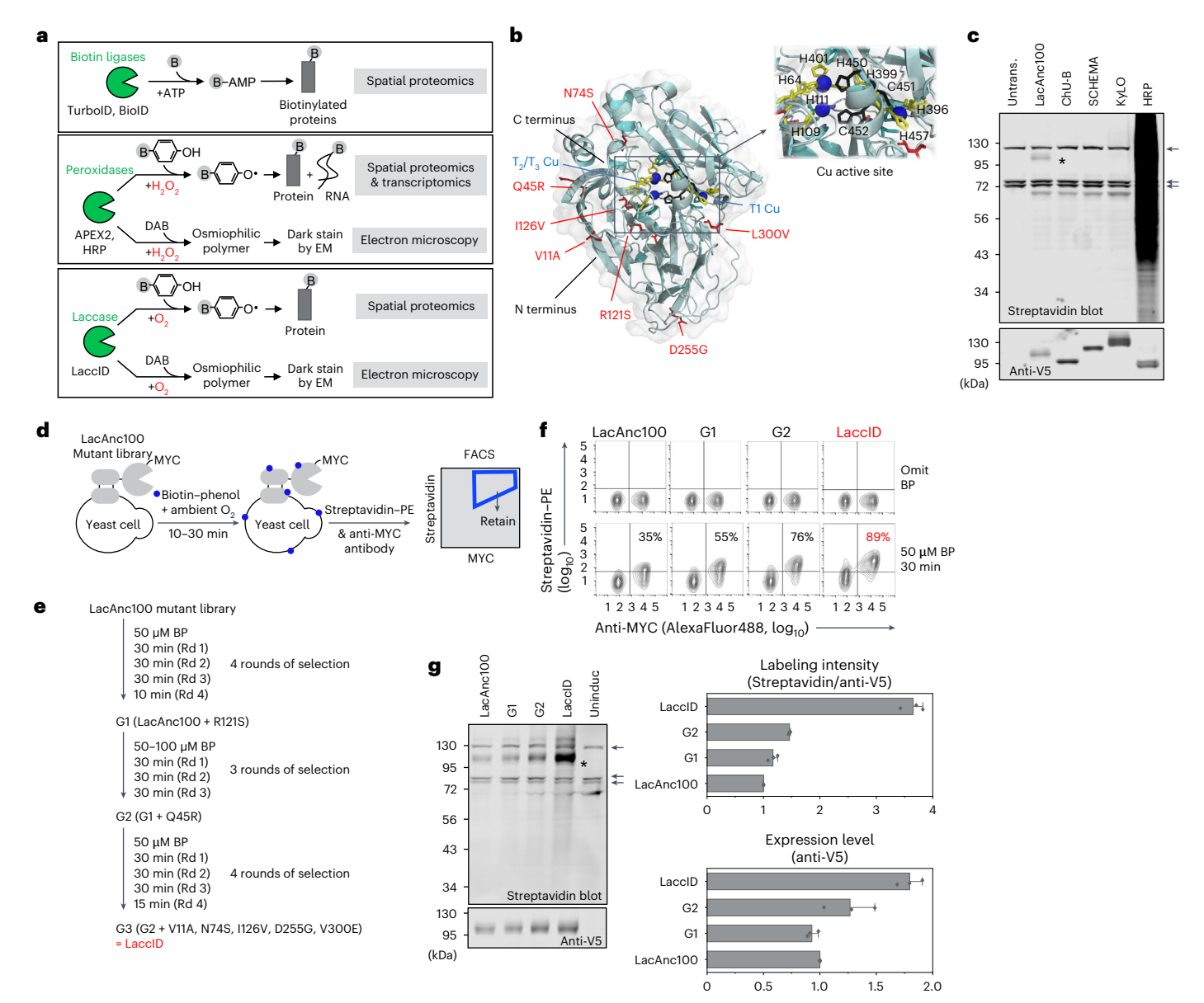


Fig. 1| **Directed evolution of LaccID. a**, LaccID is versatile, like APEX2, because it can be used for both proximity labeling and EM. LaccID is also minimally toxic, like TurboID, because it uses O_2 instead of toxic H_2O_2 . B, biotin. **b**, AlphaFold2-predicted structure of LaccID. Four copper atoms (blue) are distributed in two copper centers (one Cu atom in type I and three Cu atoms in type II and III centers). Cu-coordinating side chains (H64, H109, H111, H396, H399, H401 and H457) are shown in yellow; residues involved in electron transfer (H451, C452 and H453) are shown in black; seven mutations introduced by directed evolution are shown in red. **c**, Initial screening of four laccase templates: LacAnc100 (ref. 22), ChU-B²³, SCHEMA²⁴ and KyLO²⁵. Enzymes were fused to the transmembrane (TM) domain of human CD4 for expression on the surface of HEK293T cells. Labeling was performed for 1 h with 500 μM biotin-phenol (BP), then cell lysates were analyzed by streptavidin blotting. For comparison, HRP labeling was performed for 1 min with 500 μM BP and 1 mM H $_2O_2$. *Self-labeling of LacAnc100. Arrows point to endogenous biotinylated proteins. Untrans., untransfected. This

experiment was performed three times with similar results. ${\bf d}$, Yeast surface display selection scheme. PE, phycoerythrin. ${\bf e}$, Selection conditions used over three generations of directed evolution. The winning clone from each generation was named G1, G2 and G3, respectively. G3 is LaccID. ${\bf f}$, FACS density plots summarizing the progress of directed evolution. Yeast cells displaying LacAnc100 or G1–G3 (LaccID) were compared by labeling with 50 μ M BP for 30 min and then staining with streptavidin–PE and anti-MYC antibody. This experiment was performed three times with similar results. Percentages were calculated as a fraction of MYC $^+$ cells with streptavidin–PE staining above background. ${\bf g}$, Comparison of LacAnc100 and evolved clones on the surface of HEK293T cells. Expression of cell surface-targeted constructs was induced with doxycycline overnight and then labeling was performed for 1 h with 500 μ M BP in EBSS. *Self-labeling of LaccID. Arrows point to endogenous biotinylated proteins. Uninduc., uninduced. Right, quantification of streptavidin blot data. Data are presented as the mean values \pm s.d. of three biological replicates.

while LaccID shows stronger labeling with BMP than BP, HRP and APEX2 exhibit the opposite preference (Fig. 2c). Confocal immunofluorescence imaging confirmed the surface localization and activity of LaccID (Fig. 2d). When using BMP, cells adjacent to LaccID-expressing cells were also biotinylated to some extent (*trans*-labeling) (Fig. 2d). This *trans*-labeling was also observed on suspended K562 cells analyzed by FACS (Supplementary Fig. 4f). The BMP radical should have

a longer half-life than BP radical because of stabilization by the electron-donating methoxy group, which may result in a longer labeling radius. Consequently, for proximity labeling applications with LaccID, BMP is recommended to maximize sensitivity and BP is recommended to maximize spatial specificity.

To examine the mechanism of LaccID labeling, we generated a mutant in which the HCH motif, essential for electron transport³⁰, was

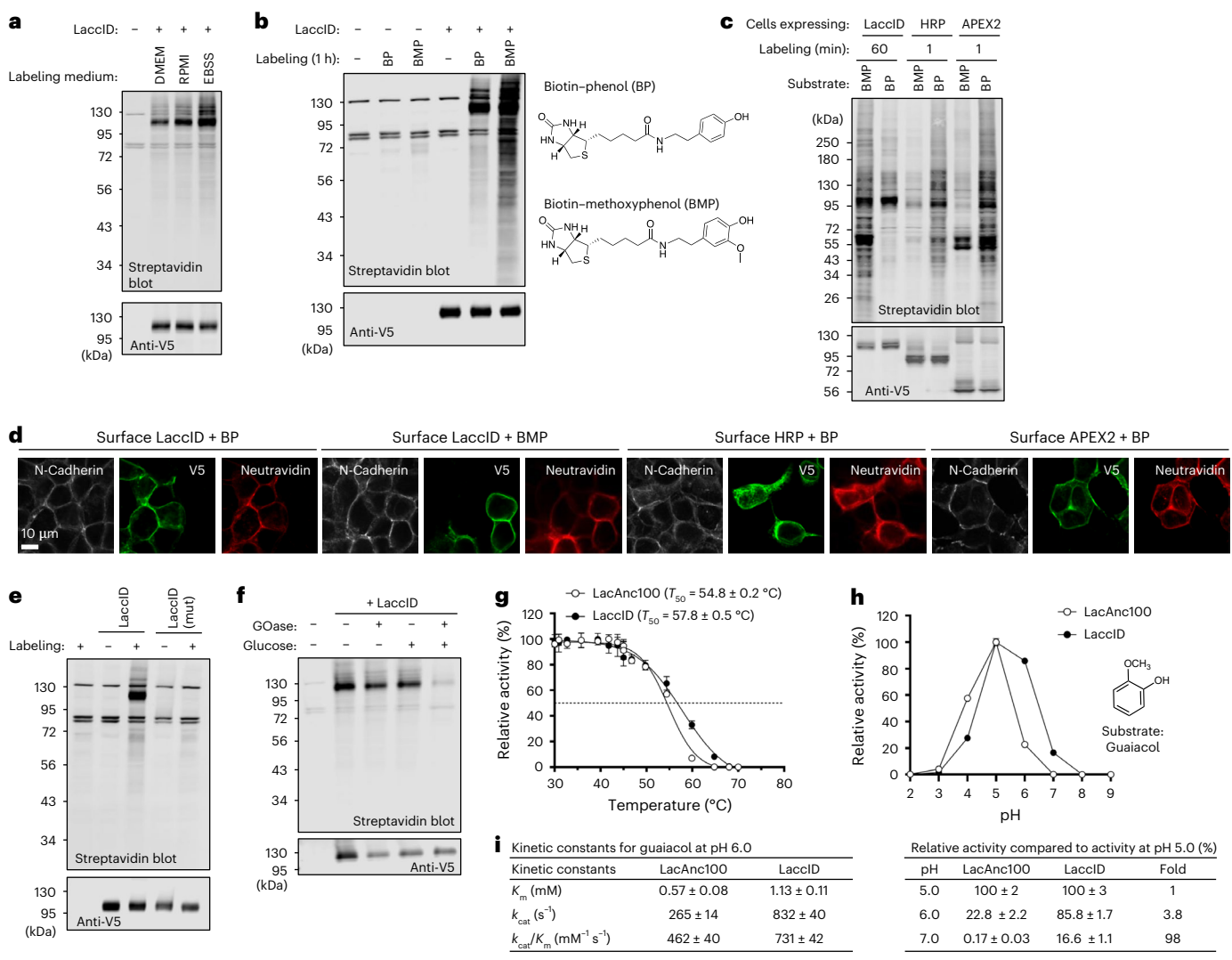


Fig. 2| **Characterization of LaccID. a**, LaccID labeling in different cell culture media. HEK293T cells expressing surface LaccID were labeled for 2 h with 500 μM BP. The molecular mass of LaccID is 53 kDa without glycosylation. This experiment was performed twice with similar results. **b**, LaccID labeling with BP versus BMP. HEK293T cells expressing surface LaccID were labeled for 1 h with 500 μM probe in EBSS. This experiment was performed three times with similar results. **c**, LaccID comparison to HRP and APEX2 on the surface of HEK293T cells. For LaccID, labeling was performed with 500 μM BP in EBSS or 500 μM BMP in RPMI. For HRP and APEX2, labeling was performed with 500 μM probe and 1 mM $\rm H_2O_2$ in DMEM. This experiment was performed twice with similar results. **d**, Confocal imaging of cells labeled as in **c**. N-cadherin is a plasma membrane marker. Neutravidin detects biotinylated proteins. Anti-V5 antibody detects enzyme expression. This experiment was performed twice with similar results. **e**, Mutations impacting the HCH motif (H450A-C451A-H452A) abolish LaccID activity. HEK293T cells expressing LaccID or mutant LaccID were labeled for 1 h with 500 μM BP in EBSS.

This experiment was performed three times with similar results. **f**, LaccID requires O_2 . HEK293T cells expressing surface LaccID were labeled with $500 \, \mu \text{M BP}$ in PBS for 1 h. Glucose oxidase (GOase) and glucose were used to deplete oxygen in the culture medium. This experiment was performed twice with similar results. **g**, Thermal stability of LacAnc100 (template) and LaccID. Purified enzymes were incubated in citrate—phosphate pH 6.0 buffer at temperatures ranging from 30 to $70\,^{\circ}\text{C}$ and then assayed for activity at pH 4.0 with ABTS substrate. The dotted line shows T_{50} . Data are presented as the mean \pm s.d. of three technical replicates. **h**, pH activity profile for LacAnc100 and LaccID. Purified enzymes were assayed with the substrate guaiacol at the indicated pH values. Conversion to product measured by absorbance at 470 nm. Additional data with other substrates (ABTS, DMP, p-coumaric acid, and sinapic acid) are presented in Supplementary Fig. 5c,d. Data are presented as the mean \pm s.d. of three biological replicates. **i**, Kinetic constants for LacAnc100 and LaccID at pH 6.0 with guaiacol. Additional data with other substrates are presented in Supplementary Fig. 5e.

changed to three alanines. As expected, this mutant abolished LaccID activity (Fig. 2e). To confirm that LaccID labeling depends on O_2 , we depleted O_2 from the labeling mixture with glucose oxidase, which consumes O_2 upon oxidation of its substrate glucose³¹. As expected, LaccID labeling decreased when both glucose oxidase and glucose were present (Fig. 2f and Supplementary Fig. 4g).

Kinetic characterization of LaccID

To further characterize the catalytic activity of LaccID, we purified recombinant enzyme from yeast *S. cerevisiae* using a protease-cleavable

His $_8$ -tag (Supplementary Fig. 5a). We first performed a thermal stability assay by incubating the enzymes at different temperatures and then measuring enzyme activities via oxidation of ABTS, a commonly-used laccase substrate ³². LaccID was more stable than our starting template LacAnc100, with a T_{50} (temperature at which the enzyme loses 50% of activity after 10 min of incubation) of 57.8 \pm 0.5 °C compared to 54.8 \pm 0.2 °C for LacAnc100 (Fig. 2g). This may explain the higher expression level of LaccID compared to LacAnc100 in HEK293T cells (Fig. 1g). There was no notable difference in pH-dependent stability between the two enzymes (Supplementary Fig. 5b).

To measure catalytic turnover, we used a broader panel of substrates: ABTS, guaiacol, 2,6-dimethoxyphenol (DMP), p-coumaric acid and sinapic acid. Initial rates were determined by measuring product generation (for ABTS, guaiacol and DMP) or substrate depletion (for p-coumaric acid and sinapic acid). We found that LaccID was 1.1-fold to 20.8-fold faster than LacAnc100 in its oxidation of these substrates at pH 7.4 (Supplementary Fig. 5c). When we measured initial rates at different pH values, we found that LacAnc100 activity dropped to 0.17% of its peak value when the pH was raised from 5.0 to 7.0. By contrast, LaccID retained 16.6% of its peak activity when the pH was raised from 5.0 to 7.0 (Fig. 2h and Supplementary Fig. 5d). We also performed quantitative kinetic measurements at pH 6.0 (pH 7.0 was not possible for technical reasons explained in Methods; Fig. 2i and Supplementary Fig. 5e) and observed improvements in both $k_{\rm cat}$ and $k_{\rm cat}/K_{\rm m}$ for LaccID compared to LacAnc100.

Lastly, we measured the sensitivity of both laccases to halides, specifically chloride. We did not detect a difference in chloride IC_{50} , the concentration at which activity was reduced by 50% (Supplementary Fig. 5f). Collectively, our in vitro measurements suggest that the improvements in LaccID result from a combination of higher thermal stability and increased turnover at physiological pH (7 to 7.4) compared to LacAnc100.

To better understand the structural basis for this activity improvement, we used AlphaFold 3 (ref. 33) to model LaccID and LacAnc100. Supplementary Fig. 6 suggests that two substitutions (N74S and R121S) give rise to structural changes that reorient the copper-coordinating side chains of H451 and H453. These changes may somehow improve the pH resistance and/or catalytic efficiency of LaccID.

LaccID activity is specific to the mammalian cell surface

In mammalian cells, LacAnc100 is active at the cell surface but fusions targeted to the cytosol, mitochondria or endoplasmic reticulum (ER) lumen are inactive (Supplementary Fig. 7a). In nature, laccases are processed through the secretory pathway, which completes the glycosylation, copper insertion and disulfide bond formation necessary to generate active enzyme; these post-translational modifications may not be available in other compartments of the cell.

To test LaccID in a similar manner, we created an ER-targeted construct by appending a KDEL ER retention sequence and prepared analogous constructs for APEX2 and HRP for comparison. Immunofluorescence staining showed correct ER localization for all constructs. with high overlap with calreticulin, an endogenous ER marker (Fig. 3a). We performed a side-by-side comparison of all ER-targeted constructs with all cell surface-targeted constructs (Fig. 3a,b). Interestingly, surface-targeted LaccID gave much cleaner localization to the cell surface than surface-targeted APEX2 or HRP, which exhibited substantial pools of trapped intracellular protein (Fig. 3a). The enhanced surface targeting of LaccID was further confirmed by antibody staining, with and without membrane permeabilization, followed by FACS analysis (Supplementary Fig. 7b). We then performed labeling with BP probe. While APEX2 and HRP both showed BP labeling on the cell surface and in the ER lumen, LaccID was exclusively active on the cell surface, with no labeling detected from ER-targeted LaccID (Fig. 3a,b).

To further examine the cell surface specificity of LaccID, we performed promiscuous labeling with BP, enriched the biotinylated proteins with streptavidin beads and blotted the enriched material with antibodies against the endogenous ER marker calreticulin and the cell surface marker N-cadherin. Figure 3c shows that surface-targeted LaccID enriches N-cadherin but not calreticulin, while surface-targeted APEX2 and HRP enrich both markers because of (1) substantial pools of APEX2 and HRP in the ER lumen because of their imperfect targeting to the cell surface, and (2) high activity of APEX2 and HRP in the ER compartment. The serendipitous discovery of LaccID's cell surface selectivity provides an opportunity for facile cell surface proteome mapping, explored below.

LaccID's inactivity in the ER may result from limited intracellular copper, which is supplied by copper chaperones localized predominantly in the Golgi³⁴. This hypothesis is supported by our observation that ER-targeted LaccID was unable to catalyze DAB polymerization after cell fixation; however, preincubation of the fixed cells with CuSO₄ restored activity (Supplementary Fig. 7c). We also generated a construct in which LaccID was targeted directly to the Golgi compartment. Golgi-LaccID did not show labeling with BP in living cells (Supplementary Fig. 7d) but did polymerize DAB in fixed cells (Supplementary Fig. 7e). Perhaps the discrepancy is due to lower oxygen availability inside living cells compared to fixed cells. We also examined the role of glycosylation by introducing asparagine-to-alanine substitutions at six different potential N-glycosylation sites in surface-targeted LacAnc100, none of which appeared to notably reduce its activity (Supplementary Fig. 7f). Together, our findings indicate that LaccID targets cleanly to the cell surface and is selectively active there, in contrast to APEX2 and HRP, which exhibit activity in ER and Golgi compartments. The cell-surface-selective activity may result from Golgi localization of copper chaperones and greater oxygen availability at the cell surface.

LaccID as a genetically encoded tag for EM

Genetically encoded labels analogous to GFP for fluorescence microscopy are highly valuable for marking organelles, proteins and other cellular features in EM. Because laccases are known to oxidize DAB¹⁵, a molecule used to generate contrast for EM¹², we tested LaccID as an EM tag (Fig. 4a).

We prepared HEK293T cells expressing cell surface-targeted LaccID, fixed the cells and overlaid them with DAB. LaccID catalyzed the oxidative polymerization and local deposition of DAB, which could be visualized by brightfield microscopy (Fig. 4b). Interestingly, the difference in activity compared to cell surface HRP and APEX2 in this context was considerably smaller than the activity difference observed for biotinylation on living cells. Possible reasons could be that (1) DAB is preferred by LaccID over other aromatic substrates, and (2) DAB labeling was performed in sodium cacodylate buffer, which does not contain laccase inhibitors such as halides and thiols.

Generating EM contrast at the cell surface delineates cell-cell borders and allows for accurate cell segmentation and synapse reconstruction 35 . For such applications, achieving efficient plasma membrane labeling while minimizing the labeling of intracellular membranes is crucial. We hypothesized that LaccID might provide more selective cell surface labeling than peroxidases on the basis of the observations above (Fig. 3). Transmission electron microscopy (TEM) imaging of OsO_4 -postfixed HEK293T cells showed that surface LaccID provides excellent contrast at the plasma membrane, with minimal staining of intracellular membranes on the ER, mitochondria and nucleus (Fig. 4c). By contrast, APEX2, also targeted to the cell surface, provided much weaker staining of the plasma membrane relative to intracellular organelles (Supplementary Fig. 8a,b).

Next, we tested the use of LaccID as an EM label in the brains of fruit fly (*Drosophila melanogaster*). We generated transgenic flies by crossing *UAS-LaccID* flies with *elav-GAL4* (pan-neuronal GAL4) flies (Fig. 4d). Confocal immunofluorescence imaging of the fly larval ventral nerve cord (VNC) confirmed neuron-specific expression of LaccID and cell surface localization at axon termini at neuromuscular junctions (NMJs) (Fig. 4e,f). TEM imaging of fixed VNCs showed dark contrast at the plasma membrane when both LaccID and Cerium-DAB2 were present (Fig. 4g and Supplementary Fig. 8c). In Supplementary Fig. 8d, cerium elemental maps showed that the dark-stained regions in EM were indeed positive for cerium atoms, which were coordinated by the DAB-chelate conjugate³⁶. These findings indicate that LaccID can serve as a peroxide-free, surface-specific, genetically encodable EM marker suitable for use in fixed cells and tissue.

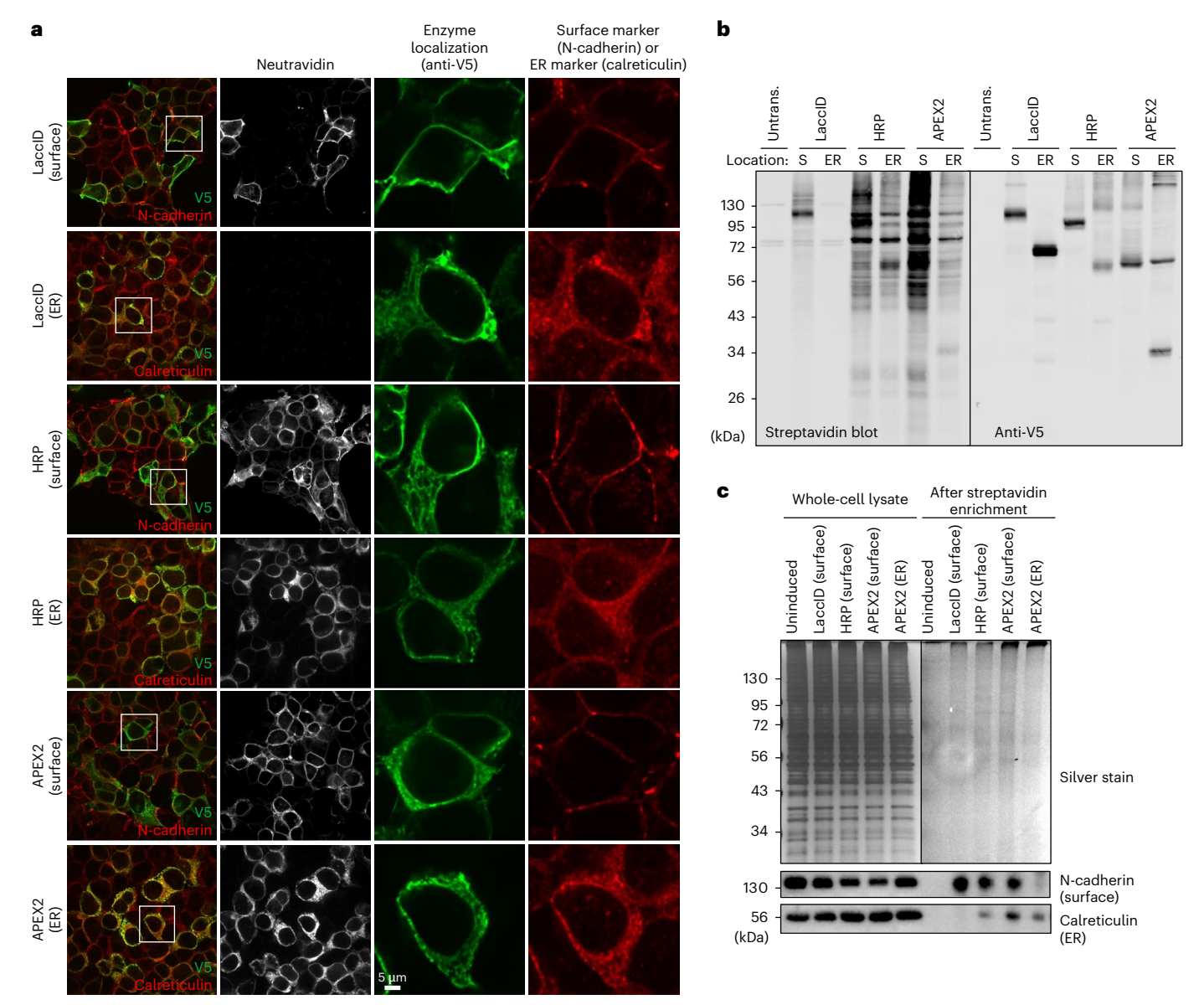


Fig. 3 | **LaccID** is selectively active on the cell surface. a, Confocal imaging of enzymes targeted to the cell surface or ER lumen of HEK293T cells. LaccID samples were labeled with BP for 1 h in EBSS. HRP and APEX samples were labeled for 1 min with BP and H_2O_2 in DMEM. The cells were then fixed and stained with anti-V5 antibody to detect expression, neutravidin–AF647 to detect biotinylated proteins and organelle markers as indicated. This experiment was performed twice with similar results. **b**, Promiscuous biotinylation activity of enzymes at the surface (S) or in the ER lumen of HEK293T cells. Cells were labeled with BP

as in **a** and then blotted with streptavidin and anti-V5 antibody. The molecular mass of APEX2 is 30.9 kDa and the higher band may be a crosslinked dimer. This experiment was performed twice with similar results. **c**, Western blot detection of proteins enriched by LaccID, HRP or APEX, targeted to the cell surface or ER lumen. Lysates from HEK293T cells labeled as in **a** were enriched with streptavidin beads and eluates were blotted for a surface marker protein (N-cadherin) or ER lumen marker protein (calreticulin). This experiment was performed twice with similar results.

LaccID for mapping cell surface proteomes

Cell surface proteomes ('surfaceomes') drive development, intercellular communication, synapse formation, immune responses and a vast array of other biological processes in multicellular organisms. Methods to map cell surface proteomes in an unbiased, comprehensive and cell-type-selective manner are increasingly needed to probe such biology. Peroxidase-mediated proximity labeling of surface proteomes in fly³7 and mouse³ have uncovered proteins that mediate nervous system development. However, these studies were limited by the toxicity of H_2O_2 and the poor tissue permeability of BxxP, a membrane-impermeant variant of BP required to prevent labeling of intracellular ER and Golgi proteins by surface-targeted HRP³. Because LaccID does not require H_2O_2 and its activity is inherently selective for

the cell surface (obviating the need for special probes such as BxxP), we wondered whether LaccID could be used for nontoxic mapping of cell-type-specific surfaceomes in complex biological settings.

We established a coculture assay to examine the interactions between human primary CD8 $^{+}$ T cells and tumor cells expressing a specific tumor antigen, NY-ESO-1 (ref. 38). The T cells were engineered to express cell surface LaccID and either a T cell receptor (TCR) or chimeric antigen receptor (CAR) against NY-ESO-1 (Supplementary Fig. 9a). The T cells were then cocultured with NY-ESO-1 and A375 tumor cells in a 3:1 ratio for 24 h before labeling with BMP for 2 h (Fig. 5a and Supplementary Fig. 9b).

A total of 18 samples were quantitatively compared using tandem mass tag (TMT)-based mass spectrometry (MS) proteomics

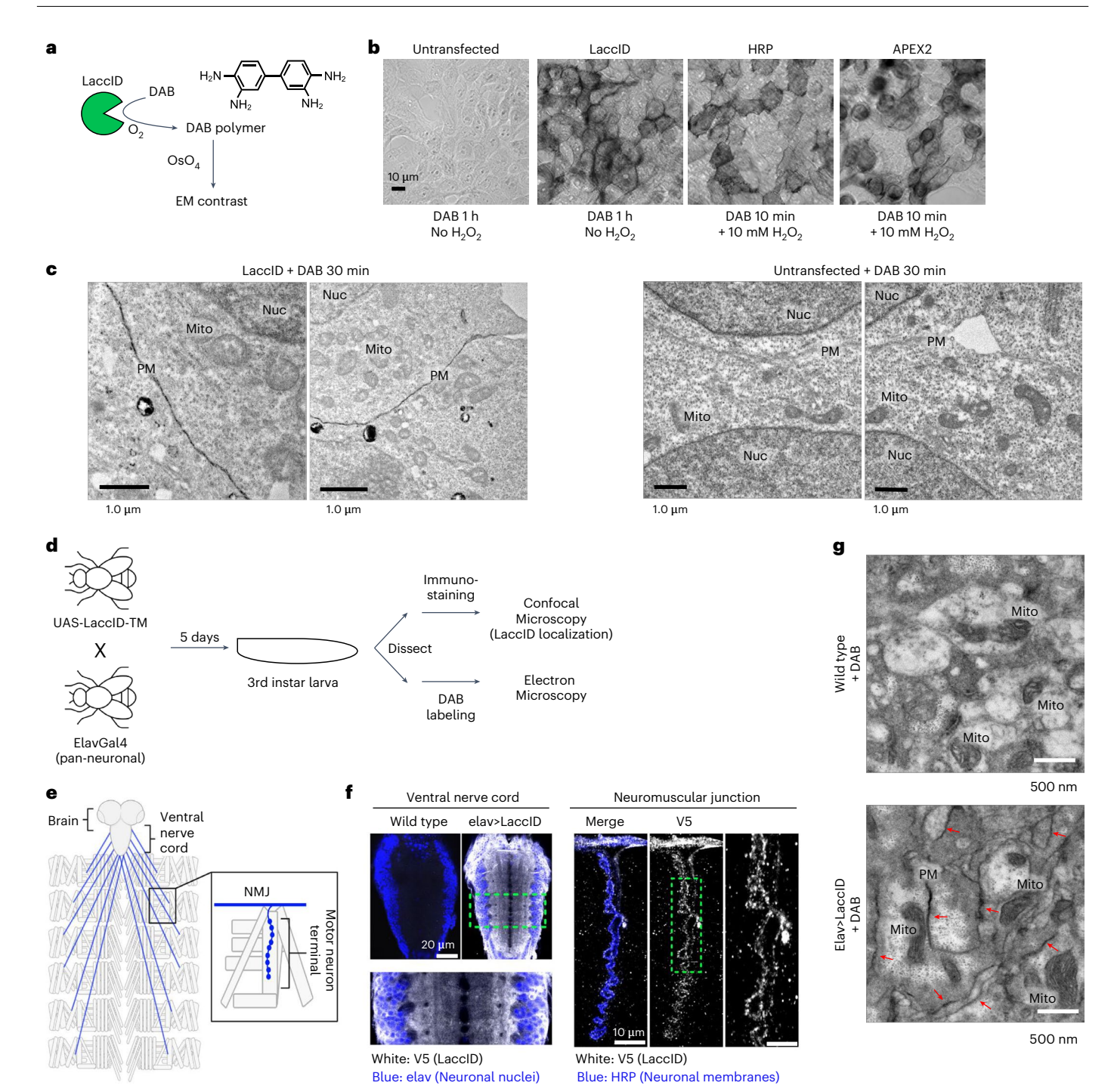


Fig. 4 | LaccID is a genetically encoded EM tag. a, LaccID generates EM contrast by catalyzing the oxidative polymerization of diaminobenzidine (DAB), which recruits electron-dense osmium that appears dark on EM micrographs.

b, LaccID-catalyzed DAB staining of fixed cells. HEK293T cells expressing surface LaccID, HRP or APEX2 were fixed using 2% (v/v) glutaraldehyde, stained with DAB for indicated times and imaged by brightfield microscopy. This experiment was performed twice with similar results. c, EM imaging of HEK293T cells expressing LaccID targeted to the cell surface through fusion to the TM domain of CD4. Cells were fixed using 2% glutaraldehyde, incubated with DAB for 30 min and then postfixed with 1% osmium tetroxide for 1 h. Images are representatives of >3 fields of view. PM, plasma membrane; Nuc, nucleus; Mito, mitochondria. Right, negative control with LaccID omitted. d, Generation of neuron-specific LaccID transgenic flies. e, Schematic of the larval *Drosophila* central nervous system and the innervation of body wall muscles by motor neuron axons. LaccID

is expressed in neurons of the brain and VNC. Inset shows motor neuron axons leaving the VNC to innervate muscles at NMJs, which are visualized by confocal microscopy in ${\bf f.f.}$ Representative confocal images of anti-V5 immunostained LaccID (epitope tagged with V5) in the VNC (left) or NMJ (right). Neuronal nuclei and membranes were labeled with anti-Elav and anti-HRP 51 , respectively. Boxed regions are magnified to show LaccID expression in neuronal cell bodies and neuropil in the VNC (left) and at a motor neuron terminal (right). This experiment was performed twice with similar results. ${\bf g.f.}$ Representative EM images of DAB-stained fly VNC. Fixed VNC tissues from fly larvae were stained with Ce-DAB2 for 75 min, followed by postfixation with 1% osmium tetroxide for 1 h. Red arrows indicate plasma membrane (PM) labeling in LaccID-expressing samples (Elav > LaccID). Additional fields of view, as well as cerium detection by EELS and EFTEM, are shown in Supplementary Fig. 8c,d. This experiment was performed once.

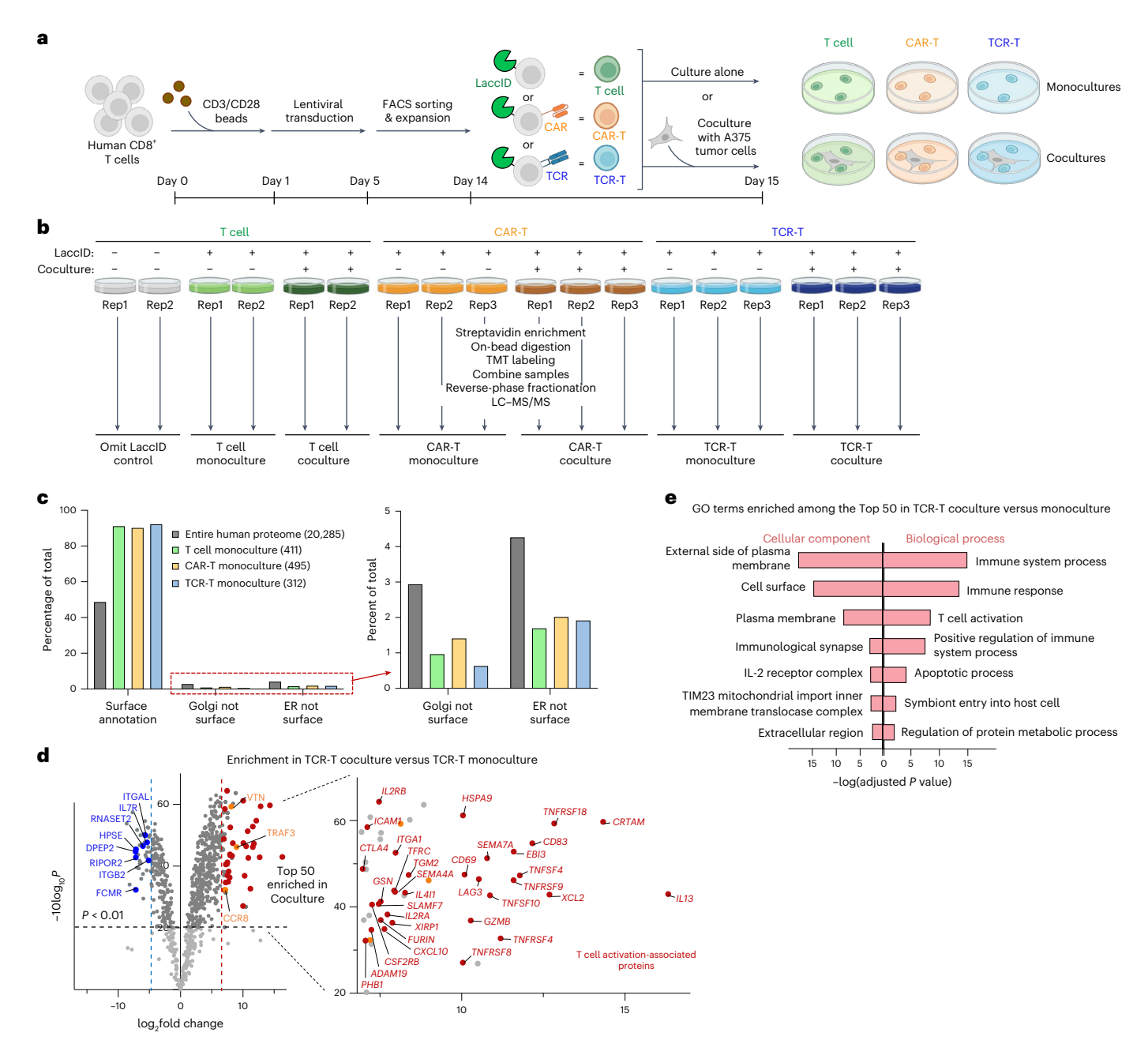


Fig. 5 | LaccID mapping of the T cell surface proteome in the presence of tumor cells. a, Cocultures were established between LaccID-expressing T cells and A375 melanoma tumor cells. The tumor cells expressed the NY-ESO-1 tumor antigen, while T cells expressed a CAR (orange) or TCR (blue) directed toward NY-ESO-1. In a control sample (green), T cells did not express CAR or TCR. This image was created with BioRender.com. b, Design of 18-plex TMT proteomic experiment. All samples were treated with BMP for 2 h before quenching, lysis and streptavidin enrichment of LaccID-labeled proteins. Controls omit TCR and CAR (T cell samples, green), omit LaccID, or are not cocultured (monoculture samples). c, LaccID enriches cell surface proteins in all three monoculture samples.

Golgi-resident and ER-resident proteins (lacking cell surface annotation) are de-enriched. ${\bf d}$, Volcano plot comparing LaccID-labeled TCR-T cell cocultures to monocultures. Proteins with previous literature connections to T cell activation are colored red, those with indirect connections are colored orange, and previously- annotated downregulated proteins are colored blue (Supplementary Table 3). ${\bf P}$ values were computed using moderated ${\bf t}$ -tests without multipletesting correction (cutoff: ${\bf P}$ <0.01). ${\bf e}$, GO terms enriched in top 50 TCR-T cell coculture versus monoculture dataset. GO enrichment analysis was performed using g:Profiler, which applies a cumulative hypergeometric test with Benjamini-Hochberg FDR correction for multiple comparisons.

(Fig. 5b). We observed a high correlation between biological replicates (Supplementary Fig. 9c) and good segregation of samples by coculture status and receptor expression according to principal component analysis (Supplementary Fig. 9d). To obtain cell surface proteome lists for T cell, CAR-T cell and TCR-T cell monocultures (grown in the absence of tumor cells), we applied a \log_2 -transformed fold change cutoff with a 5% false discovery rate (FDR), defined by the retention of cytosolic and nuclear proteins, which should

not be labeled by LaccID (Supplementary Fig. 9e). The resulting protein lists (312 to 495 in size; Supplementary Table 2 and Supplementary Fig. 9f,g) were highly enriched in cell surface proteins, with 90–92% of entries having prior cell surface annotation (Fig. 5c and Supplementary Fig. 9f). Notably, few ER-resident and Golgi-resident proteins were enriched in any of the proteomes (Fig. 5c), consistent with our observation that LaccID lacks activity in these compartments.

Coculture surfaceomes were determined in a similar manner; however, because of the higher presence of intracellular proteins (cytoskeletal proteins in the T cell and CAR-T cell cocultures and mitochondrial proteins in the TCR-T cell cocultures), we applied a less stringent cutoff (10% instead of 5% FDR) (Supplementary Fig. 10a). The intracellular proteins could reflect transfer from tumor cells to immune cells through extracellular vesicles, mitochondria–plasma membrane interactions³⁹ or tunneling nanotubes⁴⁰ or they could be artifacts from nonspecific binding due to our use of the monoculture (rather than coculture) no-LaccID negative control for data filtering (Fig. 5b). The final coculture protein lists (450–595 in size) were 76–81% specific for cell surface proteins (Supplementary Table 2 and Supplementary Fig. 10b).

Comparison of monoculture and coculture datasets showed little evidence of T cell activation for the T cell (no TCR and no CAR) samples, as expected (Supplementary Figs. 10c,e). The CAR-T cells showed activation (for example, upregulation of CD40LG, IL-2RA and CSF2RB markers) even in the absence of tumor cells (Supplementary Fig. 9g-i), consistent with previous reports of antigen-independent signaling by CARs⁴¹. Upon coculture, CAR-T cell surfaceomes did not change much (Supplementary Fig. 10d,f) because the cells were already activated and the particular CAR we used may exhibit low antigen sensitivity⁴². The greatest proteomic change was observed for TCR-T cells, which strongly upregulated many known markers of T cell activation upon coculture with tumor cells. For example, the activation markers CD69, CD83, LAG3, IL-2RA/B, TFRC, TNFRSF4/9/18 and CTLA4 were highly enriched (Fig. 5d,e). Among the top 50 hits (proteins most enriched by LaccID in TCR-T cell coculture versus monoculture) were 33 proteins with direct literature links to CD8⁺T cell activation, another 3 proteins with indirect links, 2 membrane proteases (ADAM19 and FURIN) and 8 mitochondrial proteins (Fig. 5d, Supplementary Fig. 11 and Supplementary Table 3). Additionally, we observed downregulation of several markers known to be decreased in activated T cells, including DPEP2, FCMR, RIPOR2, HPSE and RNASET2 (Fig. 5d and Supplementary Table 3).

A few unexpected proteins were present in our TCR-T cell top-50 list, raising the possibility of novel biological hypotheses. For example, prohibitin 1 (PHB1) is a ubiquitous protein expressed in multiple subcellular regions but primarily in the inner mitochondrial membrane. Perhaps our detection of PHB1 in the TCR-T cell coculture reflects tumor-induced relocalization of PHB1 from mitochondria⁴³ or other intracellular stores to the cell surface. This alteration could be driven by phosphorylation⁴⁴ and could have a role in integrating immune signaling with metabolism⁴⁵. Another protein we identified is gelsolin (GSN), a Ca²⁺-dependent actin binder that severs actin filaments. A recent report showed that GSN is secreted through exosomes from ovarian cancers and can induce T cell inhibition and apoptosis⁴⁶. A375 melanoma cells used in our experiments express GSN. Perhaps our detection of GSN in all cocultures relative to monocultures reflects GSN secretion from A375 tumor cells to facilitate immune evasion^{46,47}.

Our findings show that LaccID can be a useful tool for mapping endogenous cell surface proteomes in complex samples in a nontoxic $(H_2O_2\text{-free})$ and cell-type-specific manner.

Discussion

LaccID is an oxidizing enzyme suitable for proximity labeling and EM applications. LaccID offers unique benefits over established proximity labeling enzymes such as APEX2 and TurboID by using gentle, nontoxic (H_2O_2 -free) labeling conditions and accepting a broad range of substrate structures. In addition, LaccID can be used for selective proteome mapping at the cell surface without requiring special, membrane-impermeant substrates. This empowered us to use LaccID to map the surfaceome of T cells cocultured with tumor cells and we highlight dozens of proteins that are upregulated by TCR-antigen interaction (Fig. 5). We also used LaccID for EM imaging in the fly brain

and HEK293T cell cultures, delineating plasma membranes more clearly than peroxidase-based labels such as APEX2 (Fig. 4 and Supplementary Fig. 8). These examples showcase the promise of this new enzyme class.

LaccID was created from an ancestral fungal laccase through 11 rounds of yeast display directed evolution, which improved enzyme stability, catalytic turnover and pH activity profile to better suit physiological conditions (Figs. 1 and 2). However, the current activity of LaccID is still much lower than that of APEX2 or TurboID, requiring 1–2 h of labeling to give detectable signal, in contrast to APEX2 or TurboID, which need only 1–10 min. Future generations of LaccID may benefit from directed evolution in mammalian cells, which have different glycosylation and copper insertion machinery than yeast. In addition, selection in the presence of serum, halides and thiols could help to enrich variants that are tolerant to those species. Our current LaccID did not exhibit activity in living fly brain tissue but an improved version with in vivo activity would open the door to many proximity labeling applications.

Apart from LaccID, several antibody-based, nongenetically encoded methods have recently been reported for mapping cell surface proteomes in culture. For example, transition metal⁴⁸ and organic dye⁴⁹ photocatalysts have been conjugated to antibodies against cell surface markers to profile the microenvironment of the EGF receptor⁴⁸, the surfaceome of erythrocytes⁵⁰ and the proteome of Jurkat cell–HEK293T cell immune synapses⁴⁹. The main drawbacks of such methods are the difficulty of achieving cell type-specific profiling if suitable surface markers (that can be targeted by antibodies) are unavailable and, for future applications, the challenge of delivering large antibody reagents and high-intensity light into animals and tissue.

A major goal of connectomics is to use EM to accurately trace neurons by distinguishing cell surface membranes from intracellular membranes in thin tissue sections. LaccID provides a powerful tool with inherent selectivity for the surface membrane based on its biochemical mechanism.

Beyond proximity labeling and EM, LaccID may have utility in other areas. Engineered fungal laccases have been used for drug, food and paper production, as well as for the removal of toxic substances such as herbicides and industrial effluents²⁰. The improved thermal stability and activity of LaccID at neutral pH could prove useful in these settings. Our work paves the way for novel biological and biotechnological applications of this versatile enzyme class.

Online content

Any methods, additional references, Nature Portfolio reporting summaries, source data, extended data, supplementary information, acknowledgements, peer review information; details of author contributions and competing interests; and statements of data and code availability are available at https://doi.org/10.1038/s41589-025-01973-6.

References

- Qin, W., Cho, K. F., Cavanagh, P. E. & Ting, A. Y. Deciphering molecular interactions by proximity labeling. *Nat. Methods* 18, 133–143 (2021).
- Lam, S. S. et al. Directed evolution of APEX2 for electron microscopy and proximity labeling. Nat. Methods 12, 51–54 (2015).
- Loh, K. H. et al. Proteomic analysis of unbounded cellular compartments: synaptic clefts. Cell 166, 1295–1307.e1221 (2016).
- 4. Branon, T. C. et al. Efficient proximity labeling in living cells and organisms with TurbolD. *Nat. Biotechnol.* **36**, 880–887 (2018).
- Roux, K. J., Kim, D. I., Raida, M. & Burke, B. A promiscuous biotin ligase fusion protein identifies proximal and interacting proteins in mammalian cells. J. Cell Biol. 196, 801–810 (2012).
- Lee, S.-Y. et al. Engineered allostery in light-regulated LOV-Turbo enables precise spatiotemporal control of proximity labeling in living cells. *Nat. Methods* 20, 908–917 (2023).

- Cho, K. F. et al. Proximity labeling in mammalian cells with TurboID and split-TurboID. Nat. Protoc. 15. 3971–3999 (2020).
- Shuster, S. A. et al. In situ cell-type-specific cell-surface proteomic profiling in mice. Neuron 110, 3882–3896 (2022).
- Rhee, H. W. et al. Proteomic mapping of mitochondria in living cells via spatially restricted enzymatic tagging. Science 339, 1328–1331 (2013).
- Fazal, F. M. et al. Atlas of subcellular RNA localization revealed by APEX-Seq. Cell 178, 473–490 (2019).
- Zhou, Y. et al. Expanding APEX2 substrates for proximity-dependent labeling of nucleic acids and proteins in living cells. Angew. Chem. Int. Ed. Engl. 58, 11763–11767 (2019).
- Martell, J. D. et al. Engineered ascorbate peroxidase as a genetically encoded reporter for electron microscopy. Nat. Biotechnol. 30, 1143–1148 (2012).
- Mate, D. M. & Alcalde, M. Laccase: a multi-purpose biocatalyst at the forefront of biotechnology. *Microb. Biotechnol.* 10, 1457–1467 (2017).
- Mayer, A. M. Polyphenol oxidases in plants and fungi: going places? A review. *Phytochemistry* 67, 2318–2331 (2006).
- Zhang, X. & Flurkey, W. H. Phenoloxidases in portabella mushrooms. J. Food Sci. 62, 97–100 (1997).
- Viswanath, B., Rajesh, B., Janardhan, A., Kumar, A. P. & Narasimha, G. Fungal laccases and their applications in bioremediation. *Enzym. Res* 2014, 163242 (2014).
- Ast, T. & Mootha, V. K. Oxygen and mammalian cell culture: are we repeating the experiment of Dr. Ox? Nat. Metab. 1, 858–860 (2019).
- Cisneros, B. T. & Devaraj, N. K. Laccase-mediated catalyzed fluorescent reporter deposition for live-cell imaging. ChemBioChem 21, 98–102 (2020).
- Loi, M., Glazunova, O., Fedorova, T., Logrieco, A. F. & Mulè, G. Fungal laccases: the forefront of enzymes for sustainability. J. Fungi (Basel) 7, 1048 (2021).
- 20. Mate, D. M. & Alcalde, M. Laccase engineering: from rational design to directed evolution. *Biotechnol. Adv.* **33**, 25–40 (2015).
- Xu, F. Oxidation of phenols, anilines, and benzenethiols by fungal laccases: correlation between activity and redox potentials as well as halide inhibition. *Biochemistry* 35, 7608–7614 (1996).
- Gomez-Fernandez, B. J., Risso, V. A., Rueda, A., Sanchez-Ruiz, J. M. & Alcalde, M. Ancestral resurrection and directed evolution of fungal mesozoic laccases. *Appl. Environ. Microbiol.* 86, e00778–20 (2020).
- 23. Mate, D. M. et al. Blood tolerant laccase by directed evolution. *Chem. Biol.* **20**, 223–231 (2013).
- 24. Mateljak, I., Rice, A., Yang, K., Tron, T. & Alcalde, M. The generation of thermostable fungal laccase chimeras by SCHEMA-RASPP structure-guided recombination in vivo. ACS Synth. Biol. **8**, 833–843 (2019).
- Vicente, A. I. et al. Evolved alkaline fungal laccase secreted by Saccharomyces cerevisiae as useful tool for the synthesis of C-N heteropolymeric dye. J. Mol. Catal. B Enzym. 134, 323–330 (2016).
- Aza, P. & Camarero, S. Fungal laccases: fundamentals, engineering and classification update. *Biomolecules* 13, 1716 (2023).
- Risso, V. A., Sanchez-Ruiz, J. M. & Ozkan, S. B. Biotechnological and protein-engineering implications of ancestral protein resurrection. *Curr. Opin. Struct. Biol.* 51, 106–115 (2018).
- Bertrand, B. et al. Functional expression, production, and biochemical characterization of a laccase using yeast surface display technology. *Fungal Biol.* 120, 1609–1622 (2016).

- Suatoni, J. C., Snyder, R. E. & Clark, R. O. Voltammetric studies of phenol and aniline ring substitution. *Anal. Chem.* 33, 1894–1897 (1961).
- Bento, I. et al. Mechanisms underlying dioxygen reduction in laccases. Structural and modelling studies focusing on proton transfer. BMC Struct. Biol. 10, 28 (2010).
- 31. Swoboda, M. et al. Enzymatic oxygen scavenging for photostability without pH drop in single-molecule experiments. *ACS Nano* **6**, 6364–6369 (2012).
- 32. Johannes, C. & Majcherczyk, A. Laccase activity tests and laccase inhibitors. *J. Biotechnol.* **78**, 193–199 (2000).
- Abramson, J. et al. Accurate structure prediction of biomolecular interactions with AlphaFold 3. Nature 630, 493–500 (2024).
- 34. Polishchuk, R. & Lutsenko, S. Golgi in copper homeostasis: a view from the membrane trafficking field. *Histochem. Cell Biol.* **140**, 285–295 (2013).
- 35. Briggman, K. L. & Denk, W. Towards neural circuit reconstruction with volume electron microscopy techniques. *Curr. Opin. Neurobiol.* **16**, 562–570 (2006).
- Adams, S. R. et al. Multicolor electron microscopy for simultaneous visualization of multiple molecular species. *Cell Chem. Biol.* 23, 1417–1427 (2016).
- 37. Li, J. et al. Cell-surface proteomic profiling in the fly brain uncovers wiring regulators. *Cell* **180**, 373–386 (2020).
- 38. Thomas, R. et al. NY-ESO-1 based immunotherapy of cancer: current perspectives. *Front. Immunol.* **9**, 947 (2018).
- Montes de Oca Balderas, P. Mitochondria-plasma membrane interactions and communication. J. Biol. Chem. 297, 101164 (2021).
- Saha, T. et al. Intercellular nanotubes mediate mitochondrial trafficking between cancer and immune cells. *Nat. Nanotechnol.* 17, 98–106 (2022).
- Long, A. H. et al. 4-1BB costimulation ameliorates T cell exhaustion induced by tonic signaling of chimeric antigen receptors. *Nat. Med.* 21, 581–590 (2015).
- Burton, J. et al. Inefficient exploitation of accessory receptors reduces the sensitivity of chimeric antigen receptors. Proc. Natl Acad. Sci. USA 120, e2216352120 (2023).
- 43. Yurugi, H. et al. Expression of prohibitins on the surface of activated T cells. *Biochem. Biophys. Res. Commun.* **420**, 275–280 (2012).
- 44. Ande, S. R., Xu, Y. X. Z. & Mishra, S. Prohibitin: a potential therapeutic target in tyrosine kinase signaling. *Signal Transduct. Target. Ther.* **2**, 17059 (2017).
- 45. Xu, Y. X. Z. et al. Prohibitin plays a role in the functional plasticity of macrophages. *Mol. Immunol.* **144**, 152–165 (2022).
- Asare-Werehene, M. et al. Plasma gelsolin inhibits CD8 T-cell function and regulates glutathione production to confer chemoresistance in ovarian cancer. *Cancer Res.* 80, 3959–3971 (2020).
- Giampazolias, E. et al. Secreted gelsolin inhibits DNGR-1-dependent cross-presentation and cancer immunity. Cell 184, 4016–4031 (2021).
- Geri, J. B. et al. Microenvironment mapping via Dexter energy transfer on immune cells. Science 367, 1091–1097 (2020).
- 49. Lin, Z. et al. Multiscale photocatalytic proximity labeling reveals cell surface neighbors on and between cells. *Science* **385**, eadl5763 (2024).
- 50. Buksh, B. F. et al. µMap-Red: proximity labeling by red light photocatalysis. *J. Am. Chem.* Soc. **144**, 6154–6162 (2022).
- 51. Paschinger, K., Rendić, D. & Wilson, I. B. Revealing the anti-HRP epitope in *Drosophila* and *Caenorhabditis*. *Glycoconj. J.* **26**, 385–395 (2009).

Publisher's note Springer Nature remains neutral with regard to jurisdictional claims in published maps and institutional affiliations.

Open Access This article is licensed under a Creative Commons Attribution-NonCommercial-NoDerivatives 4.0 International License, which permits any non-commercial use, sharing, distribution and reproduction in any medium or format, as long as you give appropriate credit to the original author(s) and the source, provide a link to the Creative Commons licence, and indicate if you modified the licensed material. You do not have permission under this licence

to share adapted material derived from this article or parts of it. The images or other third party material in this article are included in the article's Creative Commons licence, unless indicated otherwise in a credit line to the material. If material is not included in the article's Creative Commons licence and your intended use is not permitted by statutory regulation or exceeds the permitted use, you will need to obtain permission directly from the copyright holder. To view a copy of this licence, visit https://creativecommons.org/licenses/by-nc-nd/4.0/.

© The Author(s) 2025

Methods

Cloning

All constructs were generated using standard cloning techniques, as previously described. In brief, gene fragments were obtained from Integrated DNA Technologies or Twist Biosciences or amplified using Q5 polymerase (New England Biolabs, M0491S). Vectors were digested using enzymatic restriction digest and ligated to either gel-purified PCR products or ordered gene fragments using Gibson assembly. Ligated plasmid products were transformed into competent XL1-Blue *Escherichia coli*. Detailed information on the constructs is provided in the Supplementary Information.

Mammalian cell culture, transfection and generation of stable cell lines

Mammalian cell cultures were performed following previously published protocols⁶. In brief, HEK293T cells (American Type Culture Collection (ATCC), CRL-3216) were cultured in complete DMEM (Gibco, 11965-092) supplemented with 10% (v/v) FBS (VWR, 97068-085) and 1%penicillin-streptomycin (VWR, 16777-164) at 37 °C under 5% CO₂. For transient expression, cells in 12-well plates were typically transfected at roughly 70% confluency using 2.5 μl of polyethyleneimine (PEI; 1 mg ml⁻¹ in water, pH7.3) or Lipofectamine 2000 (Life Technologies) and 1,000 ng of plasmid in 100 µl of serum-free medium. Stable cell lines were generated with lentivirus infection. Lentivirus was generated by transfecting HEK293T cells plated to roughly 60% confluency in a six-well dish with 250 ng of pMD2.G, 750 ng of psPAX2 and 1,000 ng of lentiviral vector containing the gene of interest with 10 µl of PEI in serum-free medium. Lentivirus-containing supernatant was collected after 48 h and filtered through a 0.45-µm filter. HEK293T cells at roughly 60% confluency were infected with crude lentivirus followed by selection with 10 μg ml⁻¹ puromycin for 1 week. To induce expression of proteins under a doxycycline-inducible promoter (pTRE3G), cells were incubated with medium supplemented with 100-200 ng ml⁻¹ doxycycline overnight.

Labeling in mammalian cells with LaccID

HEK293T cells expressing LaccID or its variants were prepared through doxycycline induction of stable cells or PEI transfection of LaccID-encoding plasmids. To perform labeling, cell culture medium was replaced with medium containing 500 μ M of probe and incubated at 37 °C. Best LaccID labeling conditions were as follows: 500 μ M BP for 1–2 h in EBSS or 500 μ M BMP for 1–2 h in RPMI. Labeling with HRP and APEX2 was performed for 1 min with 500 μ M BP or BMP. After labeling, cells were quenched with 10 mM sodium ascorbate and 5 mM Trolox in DPBS, washed three additional times with DPBS and analyzed by Western blot or immunofluorescence as described below.

LaccID labeling with various additives

For oxygen depletion experiments, labeling was performed in the presence of 4% (w/v) glucose and 0.25 mg ml $^{-1}$ glucose oxidase (Sigma-Aldrich, G2133). For BP labeling with different additives, each component was added with following concentrations: 5%, 10% and 15% FBS; 0.5%, 1% and 1.5% penicillin–streptomycin; 50, 100 and 150 mM CaCl $_2$; 0.03, 0.06 and 0.09 g l $^{-1}$ cysteine, glycine or serine.

Western blotting

Western blotting was performed as previously described $^{\circ}$. In brief, after labeling and washing, cells were lysed with radioimmunoprecipitation assay (RIPA) lysis buffer supplemented with 1× protease inhibitor cocktail (Thermo Scientific, 78429). Lysates were cleared by centrifugation at 20,000g at 4 $^{\circ}$ C for 10 min. Cleared lysates were mixed with protein-loading buffer and boiled at 95 $^{\circ}$ C for 5 min. Samples were then loaded on 10% SDS-PAGE gels, transferred onto nitrocellulose membrane and stained with Ponceau S (Sigma) to visualize total protein loading. Blots were blocked in either 5% (w/v) nonfat milk (Lab Scientific, M-0841) or 1% (w/v) BSA in 1× Tris-buffered saline with Tween (TBST)

(Teknova, T1688) for 30–60 min at room temperature, incubated with primary antibodies in TBST for 1 hat room temperature, washed three times with TBST for 5 min each, incubated with fluorophore-conjugated secondary antibodies for 30 min at room temperature, washed three times with TBST and imaged on an Odyssey CLx imager (LI-COR) or ChemiDoc XRS+ imager with Clarity western enhanced chemiluminescence blotting substrates (Bio-Rad). A list of antibodies and dilution rates is provided in the Supplementary Information. Quantification of labeling was performed with Image Studio (LI-COR).

Immunofluorescence imaging

For immunofluorescence imaging, cells were grown on 12-mm-diameter glass coverslips (VWR, 72230-01) in 24-well plates. Cells expressing LaccID were prepared as described above. After labeling, cells were gently quenched, washed three times with DPBS, fixed and permeabilized with ice-cold methanol for 10 min. Cells were washed again three times with DPBS and blocked for 1 h with 1% BSA (Fisher Scientific, BP1600-1) in TBST at 4 °C. Cells were then incubated with primary antibodies in TBST overnight at 4 °C. After washing three times with TBST, cells were incubated with fluorophore-conjugated secondary antibodies in TBST for 1 h at room temperature. Cells were washed three times with TBST and imaged.

Imaging was performed with a Zeiss Axio Observer.Z1 microscope with a Yokogawa spinning disk confocal head, Cascade IIL:512 camera, a quad-band notch dichroic mirror (405, 488, 568 and 647 nm) and 405-nm, 491-nm, 561-nm and 640-nm lasers (all 50 mW). Images were captured through \times 63 and \times 100 oil-immersion objectives for the following fluorophores: DAPI (405-nm laser excitation, 445/40-nm emission), AlexaFluor 488 (491-nm laser excitation, 528/38-nm emission), PE and AlexaFluor 568 (561-nm laser excitation, 617/73-nm emission) and AlexaFluor 647 (647-nm laser excitation, 700/75-nm emission). Image acquisition times ranged from 10 to 500 ms per channel and images were captured as the average of two or three such exposures in rapid succession. Image acquisition and processing were carried out with the SlideBook 6.0 software (Intelligent Imaging Innovations, 3i).

Yeast cell culture

Yeast cell cultures were performed as previously described⁶. In brief, *S. cerevisiae* strain EBY100 was propagated at 30 °C in SDCAA medium supplemented with 20 mg l⁻¹tryptophan. Competent yeast cells were transformed with yeast-display plasmid pCTCON2 following the Frozen EZ yeast transformation II (Zymo Research, T2001) according to the manufacturer's protocol. Successful transformants were selected in SDCAA plates and propagated in SDCAA medium. To induce protein expression, yeasts were inoculated from saturated cultures in 10% SD/GCAA (SDCAA with 90% dextrose replaced with galactose) supplemented with 100 μ M CuSO₄ overnight.

Analysis of LaccID activity on yeast surface

Yeast cells expressing surface-displayed LaccID mutants as Aga2p fusions in a pCTCON2 (ref. 6) vector were cultured overnight in SD/ GCAA medium to induce expression. Next, 6×10^6 cells (1 OD_{600} (optical density at 600 nm) = 1×10^7 cells) were transferred into PBS with 0.1% BSA (PBS-B), containing 50–100 µM BP. Cultures were then incubated at 30 or 37 °C while rotating. After BP labeling, cells were washed with 10 mM sodium ascorbate and 5 mM Trolox in PBS-B. Yeast cells were washed three times more in cold PBS-B by pelleting at 3,000g for 2 min at 4 °C and resuspending in 1 ml of cold PBS-B. Yeast cells were stained in 50 μ l of PBS-B containing anti-MYC antibody (1:400) for 1 h at 4 °C for detecting enzyme expression; then, the cells were washed three more times and stained in 50 µl of PBS-B with goat anti-chicken-AF488 and SA-PE for 40 min at 4 °C. Samples were washed for the final three times with 1 ml of PBS-B before analysis or sorting. To analyze and sort, single yeast cells were gated on a plot of forward-scatter area by side-scatter area around the clustered population (P1) on a ZE5 cell analyzer (Bio-Rad). P1 was then gated on a plot of side-scatter width

by side-scatter height around the clustered population (P2). P2 cells were then plotted to detect AF488 and PE signals. BD FACSDiva and Bio-Rad Everest were used to collect FACS data. FlowJo version 10 (BD Biosciences) was used to analyze FACS data.

Yeast directed evolution

Yeast directed evolution was performed following previously published protocols⁶. In each generation, a LacAnc100 mutant library was generated using error-prone PCR with 100 ng of template plasmid. In each generation, three libraries were generated at different levels of mutagenesis with the following primers: forward, 5′-GGAGGAGGCTCTGGTGGAGGCGGTAGCGAGGCGGAGGGTCGGCT AGCCATATG-3′; reverse, 5′-GATCTCGAGCTATTACAAGTCCTCTTCAG AAATAAGCTTTTGTTCGGATCC-3′.

PCR products were gel-purified, then reamplified for 30 more cycles under normal conditions and gel-purified again. The pCTCON2 backbone was digested with Ndel and BamHI and gel-purified as well. Next, 4,000 ng of PCR product and 1,000 ng of cut vector were mixed and dried in a DNA speed vacuum (DNA110 Savant). The dried DNA was then resuspended in 10 µl of water and electroporated into electrocompetent EBY100 yeasts. After electroporation, yeasts were rescued in 2 ml of yeast extract peptone dextrose medium and recovered at 30 °C without shaking for 1 h. Then, 1.98 ml of the culture was propagated in 100 ml of SDCAA medium while 20 µl was used to determine library size. Yeasts were diluted 100×, 1,000×, 10,000× and 100,000× and 20 μl of each dilution was plated onto SDCAA plates at 30 °C for 3 days. The resulting library size was determined by the number of colonies on the 100×,100×,1,000× and 100,000× plates, corresponding to 104, 10⁵, 10⁶ or 10⁷ transformants in the library, respectively. Libraries with different mutation levels were combined in equal volume after testing the enzyme activity to form the yeast-display library.

Directed evolution of LaccID: generation 1

For the first round of evolution, three libraries were generated using LacAnc100 as the starting template. The three libraries were generated using error-prone PCR as described above, using the following conditions to produce varying levels of mutagenesis:

Library 1: $2 \mu M$ 8-oxo-dGTP, 0.5 μM dPTP, 20 PCR cycles Library 2: $2 \mu M$ 8-oxo-dGTP, $1 \mu M$ dPTP, 20 PCR cycles Library 3: $2 \mu M$ 8-oxo-dGTP, $2 \mu M$ dPTP, 20 PCR cycles

The library sizes (approximated by number of transformants as described above) were 6×10^7 for each library. FACS analysis of the three libraries showed robust expression and a wide range of activities for all three libraries. All libraries were combined (named E1) and used as the initial population for the first round of selections. This combined library was induced as described above.

Population E1 was passaged twice and, from this culture, approximately 1.1×10^9 cells were prepared for sorting (assuming 1 OD $_{600}\approx1\times10^7$ cells) as described above with 50 μ M BP labeling for 30 min. Then, 4.8×10^8 cells were sorted by FACS. A triangular gate that collected cells positive for both anti-MYC and streptavidin was drawn and approximately 4×10^6 cells were collected (-0.8%) to give population E1R1. Subsequent rounds were performed in a similar manner, and the details of each round are outlined below.

Library	Cells prepared	Labeling	Labeling time (min)	Cells sorted by FACS	Cells collected (%)
E1R1	1.5×10 ⁸	50 μM BP	30	4.0×10 ⁷	1.7×10 ⁴ (<0.1%)
E1R2	1.5×10 ⁸	50 μM BP	30	2.9×10 ⁷	9.8×10 ³ (<0.1%)
E1R3	7.5×10 ⁷	50 µM BP	10	1.4×10 ⁷	9.2×10 ³ (<0.1%)
E1R4	7.5×10 ⁷	50 µM BP	10	1.4×10 ⁷	5.0×10 ³ (<0.1%)

After five rounds of enrichment, 24 individual clones were sequenced from E1R4 and E1R5 and unique sequences were tested in HEK293T cell surface. Clones with higher activity (quantified by streptavidin signal/anti-V5 signal) were chosen. Combining mutations in higher-activity clones did not result in increased activity. The clone with an R121S substitution showed the best activity and was named G1 (Supplementary Fig. 1).

Directed evolution of LaccID: generation 2

For the second round of evolution, three libraries were generated using G1 (LacAnc100 + R121S) as the starting template. The three libraries were generated using error-prone PCR as described above, using the following conditions to produce varying levels of mutagenesis:

Library 1: 2 µM 8-oxo-dGTP, 2 µM dPTP, 20 PCR cycles Library 2: 4 µM 8-oxo-dGTP, 1 µM dPTP, 20 PCR cycles Library 3: 8 µM 8-oxo-dGTP, 0.5 µM dPTP, 20 PCR cycles

The library sizes (approximated by number of transformants as described above) were 6×10^7 for each library. FACS analysis of the three libraries showed robust expression and a wide range of activities for all three libraries. All libraries were combined (named E2) and used as the initial population for the first round of selections. This combined library was induced as described above.

Starting from E2R1, the directed evolution was performed in two parallel branches (Supplementary Fig. 2). In the first pathway, LaccID expression level was quantified by staining with anti-chicken–AF647. In the second pathway, staining was performed with anti-chicken–AF488, to prevent bleedover of PE signal to the AF647 channel. In addition, in sorting rounds 4 and 5 of the second pathway, two reactions were performed in parallel: labeling in the absence or presence of low-concentration quenchers to prevent transcellular labeling. Libraries from parallel labeling were combined after checking the activity of each population. As previously described, after each round, a triangular gate that collected cells positive for both anti-MYC and streptavidin was drawn for sorting. Details of each round are outlined below.

Library	Cells prepared	Labeling	Labeling time (min)	Cells sorted by FACS	Cells collected (%)
Generati	ion 2: First br	anch			
E2	1.5×10 ⁹	50 μM BP	30	2.7×10 ⁸	7.7×10 ⁵ (0.3–0.4%)
E2R1	1.5×10 ⁸	50 μM BP	30	1.0×10 ⁸	2.0×10 ⁴ (<0.1%)
E2R2	1.5×10 ⁸	50μM BP	30	4.4×10 ⁷	7.8×10³ (<0.1%)
E2R3	1.5×10 ⁸	50μM BP	30	1.3×10 ⁷	3.0×10 ³ (<0.1%)
E2R4	1.5×10 ⁸	50μM BP	30	1.0×10 ⁷	4.0×10³ (<0.1%)
Generation 2: Second branch					
E2R1	1.5×10 ⁸	100 µM BP	30	3.0×10 ⁷	1.3×10 ⁴ (<0.1%)
E2R2-2	1.5×10 ⁸	100 µM BP	30	2.0×10 ⁷	1.0×10 ⁴ (<0.1%)
E2R3-2	1.5×10 ⁸	50 µM BP	20	1.5×10 ⁷	1.5×10 ⁴ (<0.1%)
		100 µM BP+ 1/500 Q ^a	30	1.5×10 ⁷	1.4×10 ⁴ (<0.1%)
E2R4-2	1.5×10 ⁸	50μM BP	10	1.4×10 ⁷	1.4×10 ⁴ (<0.1%)
		100 µM BP+ 1/100 Q ^a	30	1.4×10 ⁷	1.4×10 ⁴ (<0.1%)

^a1× Q (quencher) is 10 mM sodium ascorbate and 5 mM Trolox.

A total of 20 individual clones were sequenced from E2R4, E2R5, E2R3-2, E2R4-2 and E2R5-2. Unique sequences were tested in HEK293T cell surface. Clones with higher activity (quantified by streptavidin signal/anti-V5 signal) were chosen. Combining mutations in higher-activity clones did not result in increased activity. Clone with a Q45R substitution showed the best activity and was named G2 (Supplementary Fig. 2).

Directed evolution of LaccID: generation 3

For the third round of evolution, three libraries were generated using G2 (LacAnc100 + Q45R;R121S) as the starting template. The three libraries were generated using error-prone PCR as described above, using the following conditions to produce varying levels of mutagenesis:

Library 1: 30 μ M 8-oxo-dGTP, 1 μ M dPTP, 20 PCR cycles Library 2: 20 μ M 8-oxo-dGTP, 2 μ M dPTP, 20 PCR cycles Library 3: 10 μ M 8-oxo-dGTP, 3 μ M dPTP, 20 PCR cycles

The library sizes (approximated by number of transformants as described above) were 6×10^7 for each library. FACS analysis of the three libraries showed robust expression and a wide range of activities for all three libraries. All libraries were combined (named E3) and used as the initial population for the first round of selections. This combined library was induced as described above. Details of each round are outlined below.

Library	Cells prepared	Labeling	Labeling time (min)	Cells sorted by FACS	Cells collected (%)
E3	1.1×109	50 μM BP	30	4.2×10 ⁸	3.4×10 ⁶ (~1%)
E3R1	1.5×108	50 μM BP	30	4.5×10 ⁷	6.0×10 ⁴ (~0.3%)
E3R2	1.5×108	50 μM BP	30	3.0×10 ⁷	3.4×10 ⁴ (~0.1%)
E3R3	1.5×108	50 μM BP	15	2.4×10 ⁷	1.1×10 ⁴ (<0.1%)
E3R4	1.5×108	50 μM BP	15	2.4×10 ⁷	1.0×10 ⁴ (<0.1%)

A total of 20 individual clones were sequenced from E3R3, E3R4 and E3R5. Unique sequences were tested in HEK293T cell surface. Clones with higher activity (quantified by streptavidin signal/anti-V5 signal) were chosen. Among four clones that showed high activity, combining mutations in three clones resulted in an increased activity. The mutant with G2 mutations + mutations from all three clones was named G3, which was subsequently named LaccID (Supplementary Fig. 3).

K562 cell culture and coculture trans-labeling experiments

K562 cells were cultured in RPMI1640 medium supplemented with 10% (v/v) FBS and 1% penicillin–streptomycin at 37 °C under 5% CO $_2$. Cells were routinely passaged in fresh cell culture medium to keep the cell density under 1.0×10^6 cells per ml. Cell lines stably expressing cytosolic GFP and surface LaccID were achieved by lentivirus infection, followed by FACS sorting.

For BMP labeling, cells were harvested from culture medium and resuspended in RPMI containing 500 μ M BMP with a final density of 9.0×10^{s} cells per ml. After 2 h of labeling at 37 °C, cells were washed and stained following the same protocol used for yeast labeling. For coculture experiments, a 1:1 mixture of wild-type K562 cells and GFP $^{+}$ cells expressing surface LaccID were labeled and analyzed in the same manner.

Cloning of His-tagged laccase variants for large-scale production

DNA sequences encoding LacAnc100 and LaccID were in vivo cloned into *S. cerevisiae* strain BJ5465. To promote in vivo recombination in yeast, the genes were PCR-amplified to introduce specific overhangs of 40–55 bp to the linearized vector using iProof high-fidelity polymerase (Bio-Rad, 1725301) following the manufacturer's specifications. The PCR products were gel-extracted, purified and cleaned (Macherey-Nagel, 740609) and 200 ng of each laccase mutant gene was transformed along with 100 ng of linearized vector into *S. cerevisiae* using a yeast transformation kit (Merck, YEAST1). The linearized vector was a modified version of pJRoC30 vector (a gift from F. H. Arnold) containing a C-terminal HRV-3C protease cleavage site (3C-tag: LEVLFQGP) followed by a GSG linker and 8×His tag. Transformed cells were plated on SDCAA dropout plates and incubated for 3 days at 30 °C. Subsequently, the selected clones were subjected to screening

for laccase activity in 96-well microtiter plates before confirmation of plasmid sequence.

Individual clones containing LacAnc100 and LaccID were inoculated into 50 µl of SC minimal medium containing 6.7 g l⁻¹ yeast nitrogen base (BD, 291940), 1.92 g l⁻¹ yeast synthetic dropout medium supplement without uracil (Merck, Y1501), 20 g l⁻¹ D-raffinose (Merck, R0250) and 25 μg ml⁻¹ chloramphenicol (Merck, C0378) in a sterile 96-well plate (Enzyscreen, CR1496c). In the plate, two columns were inoculated with LacAnc100 and LaccID and two additional columns were used for a negative control plasmid (encoding for a nonrelated protein). The plates were sealed with AeraSeal films (Merck, A9224) to allow gas exchange in cultures and incubated at 30 °C, 225 rpm and 80% relative humidity in a humidity shaker (Minitron, INFORS). After 48 h, 160 µl of expression medium (10 g l⁻¹ veast extract (Gibco, 212750), 20 g l⁻¹ peptone (Gibco, 211677), 20 g l⁻¹ D-galactose (Panreac, A1131), 67 mM potassium phosphate monobasic buffer pH 6.0 (Thermo Scientific, 424200250), 25 g l⁻¹ ethanol (Scharlau, ET00062500), 2 mM copper sulfate (Merck, C7631) and 25 μg ml⁻¹chloramphenicol (Merck, C0378)) was added to each well. The plate was further incubated for 24 h. Then, the plate was centrifuged for 15 min at 4,000g and 4 °C (Eppendorf, 5810R) and replicated with the help of a liquid handler robotic station (Freedom Evo, TECAN) by transferring 20 µl of supernatant into a new replica plate. Next, 180 µl of reaction buffer containing 100 mM citrate-phosphate buffer pH 4.0 and 1 mM ABTS (Panreac, A1088) as a substrate was added using a Multidrop robot (Multidrop Combi, Thermo Scientific). The plate was stirred briefly and laccase activity was determined following the absorption of ABTS oxidation at 418 nm (ε of ABTS⁺⁺ = 36,000 M⁻¹ cm⁻¹) in kinetic mode using a plate reader SpectraMax ABS Plus (Molecular Devices).

An aliquot from the wells containing the most active LacAnc100 and LaccID clones was inoculated in 3 ml of YPD (10 g l⁻¹ yeast extract (Gibco, 212750), 20 g l⁻¹ peptone (Gibco, 211677), 20 g l⁻¹ D-glucose (Thermo Scientific, 410955000) and 25 μg ml⁻¹ chloramphenicol (Merck, C0378)) and incubated at 30 °C and 225 rpm for 24 h. Next, recovery of laccase-containing plasmids from these cultures was performed using a Zymoprep yeast plasmid miniprep kit (Zymo Research, D2001) following the manufacturer's specifications. Zymoprep product containing shuttle vectors was transformed into E. coli XL1-Blue competent cells (Stratagene) and plated on Luria-Bertani (LB)-ampicillin plates. Single bacterial colonies were inoculated into 5 ml of LB-ampicillin medium and grown overnight at 37 °C with 250 rpm shaking (Minitron, INFORS). The plasmids were then extracted by a NucleoSpin plasmid kit (Macherey-Nagel, 740588) and sent for sequencing (Eurofins genomics). Plasmids encoding laccase variants were sequenced with the following primers: RMLN, 5'-CCTCTATACTTTAACGTCAAGG; RMLC, 5'-GCTTACATTCACGC CCTCCC; Lac seq 1F, 5'-ACAACTTCACTGTCCCGGAT; Lac seq 2F, 5'-ACCCTACAACGACCCAAACA. Verification of laccase sequences was carried out using Snapgene v6 software.

Recombinant laccase variant expression and purification

A single colony from *S. cerevisiae* transformed with LacAnc100 or LacclD was used to inoculate 30 ml of SC minimal medium supplemented with raffinose (in a 100-ml flask) and incubated for 48 h at 30 °C and 220 rpm (Orbitron shaker, INFORS). Then, the OD₆₀₀ of these precultures was measured and fresh cultures were prepared in 120 ml of SDCAA medium in a 250-ml flask (OD₆₀₀ = 0.3). They were incubated until two growth phases were completed (10–12 h, OD₆₀₀ = 1); thereafter, 50 ml of precultures were induced with 450 ml of expression medium (10 g l⁻¹ yeast extract (Gibco, 212750), 20 g l⁻¹ bacto peptone (Gibco, 211677), 20 g l⁻¹ D-galactose (Panreac, A1131), 67 mM potassium phosphate monobasic buffer pH 6.0 (Thermo Scientific, 424200250), 25 g l⁻¹ ethanol (Scharlau, ET00062500), 2 mM copper sulfate (Merck, C7631) and 25 μ g ml⁻¹ chloramphenicol (Merck, C0378)) in a 2.5-l baffled flask (Quimigen, 931136-B) (OD₆₀₀ = 0.1). The cultures were incubated

for 5 days at 30 °C and 130 rpm (Multritron, INFORS) using AeraSeal films (Merck, A9224) on top of the flask, Next, the cells were pelleted by centrifugation at 4,500g for 10 min at 4 °C (high-speed centrifuge CR22N, Eppendorf). The supernatant was collected and doubly filtered (with a glass filter and then with a PVDF filter). Clarified cell-free extracts were purified by immobilized-metal affinity chromatography. Ni-NTA agarose resin (Qiagen, 30210) was equilibrated in buffer A (20 mM Tris-HCl pH 8.0 and 150 mM NaCl) and His-tagged laccases were bound to the resin. Nonspecific bound proteins were washed out with buffer A supplemented with 25 mM imidazole (Thermo Scientific, A10221) and laccases were eluted with buffer A containing 250 mM imidazole. The eluted proteins were dialyzed against buffer A using an Amicon Ultra-15 device with a molecular cutoff of 10 kDa (Millipore, UFC901008) and concentrated to 0.5 ml. Next, proteins were treated with 3C-HRV protease (Genescript, Z03092) overnight at 4 °C without shaking according to the manufacturer's instructions. The following day, Ni-NTA resin equilibrated in buffer A was added over the cleaved laccase samples and incubated at 25 °C and 1,000 rpm in a thermomixer comfort shaker (Eppendorf) for 4 h. Samples were spun down at 1,000g for 5 min at 4 °C and the supernatant containing tag-free laccases was collected. Resin containing His-tagged 3C-HRV, noncleaved laccases and cleaved tags was discarded. Laccase purity and integrity were analyzed by SDS-PAGE using TGX 4-20% precast gels (Bio-Rad, 4561094) and protein concentrations were estimated using the Bio-Rad protein reagent adapted to 96-well microtiter plates (Bio-Rad, 5000006). Purified laccases were stored at 4 °C for further analysis.

Kinetic parameters

Steady-state kinetics constants were estimated with purified laccase variants for ABTS (Panreac, A1088), DMP (Merck, D135550), guaiacol (Thermo Scientific, 120192500) and sinapic acid (Apollo Scientific, BIS8112) in 100 mM sodium phosphate-citrate buffer pH 5.0 or 6.0. We were unable to measure the kinetic parameters at pH 7.0 because of the impractical amount of recombinant enzyme required for the assay. The concentrations ranged from 0.001 to 10 mM for ABTS, from 0.02 to 24 mM for DMP, from 0.2 to 60 mM for guaiacol and from 0.025 to 0.35 mM for sinapic acid. The data were fitted to a nonlinear substrate inhibition model $(y = V_{\text{max}} \times x / (K_{\text{m}} + x(1 + x / K_{\text{i}}))$. The catalytic efficiency (k_{cat}/K_m) was obtained by plotting turnover rates (s^{-1}) versus substrate concentrations and fitting it to the equation $y = \text{catEff} \times x/$ $(1 + InvK_m \times x(1 + x/K_i))$, where catEff is the catalytic efficiency and $InvK_m$ is $1/K_m$. Enzymatic reactions were performed in 96-well plate format (Greiner Bio-One, 655101) with 190 µl of reaction mix and 10 µl of enzymes diluted in 10 mM sodium phosphate buffer pH 7.0 at the following concentrations: 1.36 µg ml⁻¹ (LacAnc100) and 0.81 µg ml⁻¹ (LaccID) for ABTS, 1.7 µg ml⁻¹ (LacAnc100) and 0.81 µg ml⁻¹ (LaccID) for DMP and guaiacol and 6.8 µg ml⁻¹ (LacAnc100) and 8.1 µg ml⁻¹ (LaccID) for sinapic acid. For measurements with sinapic acid, 96-well plates were ultraviolet (UV)-transparent microplates (Corning, 3635). Reactions were run at room temperature in triplicate and the following molar absorption coefficients were used: ABTS, $\varepsilon_{418 \text{ nm}} = 36,000 \text{ M}^{-1} \text{ cm}^{-1}$; DMP, $\varepsilon_{469 \text{ nm}} = 27,500 \text{ M}^{-1} \text{ cm}^{-1}$; guaiacol, $\varepsilon_{470 \text{ nm}} = 12,100 \text{ M}^{-1} \text{ cm}^{-1}$; sinapic acid, $\varepsilon_{312 \text{ nm}} = 17,600 \text{ M}^{-1} \text{ cm}^{-1}$; p-coumaric acid, $\varepsilon_{300 \text{ nm}} = 17,200 \text{ M}^{-1} \text{ cm}^{-1}$. Kinetic constants were determined using 65 kDa for the molecular weight of laccase estimated by matrix-assisted laser desorption/ionization time-of-flight (MALDI-TOF) MS²². Data were analyzed with Graph-Pad Prism (version 9.5.1) and are presented as the mean \pm s.d.

Thermostability (T_{50})

The kinetic thermostability of purified LacAnc100 and LaccID was estimated by assessing their T_{50} values using 96-well gradient thermocyclers (T100 thermal cycler, Bio-Rad). Appropriate dilutions of enzymes were prepared such that 20- μ l aliquots of enzymes in reaction mix produced a linear response in kinetic mode in the spectrophotometric read. A temperature gradient was set in the thermocycler for

LacAnc100 and LaccID ranging from 30 to 70 °C as follows (in °C): 30.0, 30.9. 32.7. 35.8. 39.4. 41.8. 43.7. 45.0. 46.8. 49.8. 54.4. 59.9. 64.8. 68.0 and 70.0. Then, 50 µl of enzyme dilutions were incubated for 10 min at each temperature point into nonskirted 96-well PCR plates (VWR, 732-2387) sealed with thermoresistant adhesive sheets (Thermo Scientific. AB-0558). After this 10-min incubation, samples were immediately chilled out on ice for 10 min and further incubated at room temperature for 5 min. Then, the PCR plates were briefly spun down in a PCR-plate centrifuge (VWR) and 20 µl was transferred into a new flat-bottom 96-well plate with the help of a liquid handler (Freedom Evo, TECAN). The laccase activity was measured by adding 180 µl of reaction mixture (100 mM citrate-phosphate buffer pH 4.0 and 1 mM ABTS) by using a Multidrop robot (Multidrop Combi, Thermo Scientific). The plates were briefly stirred and activity was monitored at 418 nm in kinetic mode using a plate reader SpectraMax ABS Plus (Molecular Devices). The maximum laccase activity detected at 32.7 °C was defined as 100% (initial activity) and other temperature points were normalized to that activity (relative activity). The T_{50} value was defined as the temperature that reduced laccase activity by 50% of its initial activity after 10 min of incubation. Thermostability reactions were measured in three biological replicates. Data were analyzed with GraphPad Prism (version 9.5.1) and are presented as the mean \pm s.d. (as a percentage).

pH activity profiles

Appropriate dilutions of purified laccase variants were prepared such that 10-µl aliquots of enzymes in reaction mix gave rise to a linear response in kinetic mode for each substrate assayed. Reaction mixtures were prepared in 100 mM Britton and Robinson buffer at different pH values (2.0, 3.0, 4.0, 5.0, 6.0, 7.0, 8.0 and 9.0) containing ABTS (1 mM), DMP (5 mM), guaiacol (50 mM), sinapic acid (0.35 mM) or p-coumaric acid (0.1 mM) in each case. Then, 190 µl of reaction mixtures were added into flat-bottom 96-well plates (Greiner Bio-One, 655101), except for sinapic acid and p-coumaric acid measurements that were in UV-transparent microplates (Corning, 3635), with a Multidrop robot (Multidrop Combi, Thermo Scientific). Plates were preloaded with 10 µl of laccase dilutions prepared in 20 mM citrate-phosphate buffer pH 7.0 as follows: $0.28 \,\mu g \, ml^{-1}$ (LacAnc100) and $0.36 \,\mu g \, ml^{-1}$ (LaccID) for ABTS, 1.4 μg ml⁻¹ (LacAnc100) and 1.8 μg ml⁻¹ (LaccID) for DMP, 3.4 μg ml⁻¹ (LacAnc100) and 4.0 μg ml⁻¹ (LaccID) for guaiacol, 1.7 µg ml⁻¹ (LacAnc100) and 8.1 µg ml⁻¹ (LaccID) for sinapic acid and 340 μ g ml⁻¹(LacAnc100) and 405 μ g ml⁻¹(LaccID) for *p*-coumaric acid. The plates were briefly stirred and activity was spectrophotometrically determined (SpectraMax ABS Plus, Molecular Devices) at room temperature in kinetic mode at the specific wavelength for each substrate (described above). The relative activities at each pH value (expressed as percentages) were normalized to the maximum activity observed for each variant in the assay. Data were analyzed using GraphPad Prism (version 9.5.1) and are presented as the mean \pm s.d. (as a percentage) of three biological replicates.

pH stability profiles

Appropriate dilutions of purified laccase variants were prepared such that 20-µl aliquots of enzymes in reaction mix gave rise to a linear response in kinetic mode. Then, 5 µl of laccase variants (3.4 µg ml $^{-1}$ of LacAnc100 and 4.0 µg ml $^{-1}$ of LaccID) were incubated in a 1-ml final volume containing 100 mM Britton and Robinson buffer at different pH values (2.0, 3.0, 4.0, 5.0, 6.0, 7.0, 8.0 and 9.0) in a 96-deep well plate (Sarstedt, 82.1972) covered with a lid. The plate was stirred and stored in fridge at 4 °C during the experiment. Aliquots of 20 µl were taken from every pH value at different time points (1, 4, 48, 96 and 144 h) and added over 180 µl of 20 mM Britton and Robinson buffer at pH 7.0, which was preloaded in a flat-bottom 96-well microtiter plate (Greiner Bio-One, 655101). The plate was stirred and 20 µl of the mix was transferred to a new 96-well microtiter plate. Then, 180 µl of reaction mix (100 mM citrate–phosphate buffer pH 4.0 and 1 mM ABTS) were added

using a Multidrop robot (Multidrop Combi, Thermo Scientific) and laccase activity was measured at room temperature in a plate reader SpectraMax ABS Plus (Molecular Devices) at 418 nm. Laccase activity at every time point was normalized to the activity value of each variant at time 1 h at pH 8.0, where the maximum laccase activity was observed. Data were analyzed using GraphPad Prism (version 9.5.1) and are presented as the mean \pm s.d. (as a percentage) of three technical replicates.

Determination of initial turnover number

The initial turnover rates were determined in PBS at pH 7.4 (8 g l⁻¹ NaCl (Labkem, SOCH-00T), 1.44 g l⁻¹Na₂HPO₄ (Supelco, 1.06586), 0.2 g l⁻¹KCl (Panreac, 131494) and 0.24 g l⁻¹KH₂PO₄ (Fisher Scientific, BP362)) using ABTS (1 mM), DMP (5 mM), guaiacol (50 mM), sinapic acid (0.35 mM) or p-coumaric acid (0.1 mM) as substrate. Then, 10 ul of LacAnc100 or LaccID was added to flat-bottom 96-well plates (Greiner Bio-One, 655101) and 190 µl of reaction mixtures containing PBS and different substrates were added with the help of a Multidrop system (Multidrop Combi, Thermo Scientific). For sinapic acid and p-coumaric acid measurements, 96-well plates were UV-transparent microplates (Corning, 3635). Plates were stirred and laccase activity was assayed at room temperature in a plate reader SpectraMax ABS Plus (Molecular Devices). The absorbance was followed during initial time points, where the reaction was still linear for every substrate. Initial turnover number was defined as μmol of product μmol enzyme⁻¹ min⁻¹ using 65 kDa for the molecular mass of laccase estimated by MALDI-TOF MS²². Data were analyzed using GraphPad Prism (version 9.5.1) and are presented as the mean \pm s.d. of three technical replicates.

Inhibition in the presence of chloride

The inhibitory effect of chloride on laccase activity was estimated using ABTS at the optimum pH activity for this substrate (pH 4.0). Inhibition was determined by the IC $_{50}$ value, representing the chloride concentration that reduced 50% the initial laccase activity. Laccase activities were measured using 190 μ l of reaction mixtures (100 mM citrate–phosphate buffer pH 4.0 and 1 mM ABTS) in the presence and the absence of a gradient of NaCl (5–190 mM) and 10 μ l of purified LacAnc100 (0.34 μ g ml $^{-1}$) or LacclD (0.40 μ g ml $^{-1}$) in flat-bottom 96-well plates (Greiner Bio-One, 655101). The plates were briefly stirred and the absorbance was monitored in kinetic mode in a plate reader SpectraMax ABS Plus (Molecular Devices). The activity of laccase in the presence of NaCl was normalized to the activity in the absence of NaCl for each laccase variant. Data were analyzed using GraphPad Prism (version 9.5.1) and are plotted as the mean \pm s.d. (as a percentage) of three technical replicates.

Preparation of DAB-stained HEK293T cells for EM

LaccID-expressing cells were fixed using warm 2% glutaraldehyde in buffer (100 mM sodium cacodylate with 2 mM CaCl $_2$, pH 7.4) and then quickly moved to ice. After 1 h, cells were washed five times for 2 min each on ice with cold buffer and blocked for 5 min with cold 20 mM glycine in cold buffer. A freshly diluted solution of 0.5 mg ml $^{-1}$ DAB tetrahydrochloride in buffer was added to cells for at least 30 min at room temperature. The cells were then washed five times for 2 min each with cold buffer.

Cells expressing HRP or APEX2 were fixed and washed as described above. A freshly diluted solution of 0.5 mg ml $^{-1}$ DAB tetrahydrochloride with 10 mM $\rm H_2O_2$ in buffer was added to cells for 1–10 min at room temperature.

DAB staining and preparation of cultured cells for EM

The fixative was removed and cells were washed (five times for 1 min) with 0.1 M sodium cacodylate (Ted Pella, 18851) buffer at pH 7.4 containing 2 mM CaCl $_2$ on ice and blocked with 20 mM glycine in 0.1 M sodium cacodylate buffer pH 7.4 containing 2 mM CaCl $_2$ for 20 min on ice. Cells with APEX2 or HRP were enzymatically reacted with 2.5 mM

DAB (Sigma-Aldrich, D8001-10G) with 4 mM H₂O₂ (from 30% stock) in 0.1 M sodium cacodylate buffer at pH 7.4 for 3-20 min until the desired brown intensity color of the precipitate was visible. Cells with laccase were enzymatically reacted with DAB in 0.1 M sodium cacodylate buffer at pH 7.4 for 3-20 min until the desired brown intensity color was achieved). The cells were then washed (five times for 2 min each) with 0.1 M sodium cacodylate buffer pH 7.4 on ice and were postfixed with 1% osmium tetroxide (EMS, 19150) in 0.1 M sodium cacodylate buffer pH 7.4 for 30 min on ice. Postfixative was removed and cells were washed (five times for 1 min each) with 0.1 M sodium cacodylate buffer pH 7.4 containing 2 mM CaCl₂ on ice and then washed (five times for 1 min each) with cold double-distilled H₂O (ddH₂O) on ice. Cells were dehydrated with an ethanol series (20%, 50%, 70%, 90% and 100%) on ice for 1 min each and then 100% dry ethanol at room temperature three times for 1 min each, infiltrated with 50:50 dry ethanol: Durcupan ACM resin (Sigma-Aldrich, 44610) for 30 min and then four changes of Durcupan at 1 h each and finally embedded in a vacuum oven at 60 °C for 72 h.

Drosophila stocks and generation of UAS-HA-V5-LaccID flies

Flies were maintained on standard cornmeal medium on a 12-h lightdark cycle at 25 °C.

UAS-HA-V5-LaccID flies were generated from gBlocks containing a wingless signal peptide upstream of two epitope tags (HA and V5) followed by Posophila codon-optimized LaccID fused to CD2. These gBlocks were cloned into a 10x pUASt-attB vector, validated by Sanger sequencing and injected into embryos bearing an attP40 landing site. G_0 flies were crossed to a white–balancer and all white+ progeny were individually balanced.

Drosophila immunofluorescence and image acquisition

Wandering third-instar larvae (L3) were obtained by crossing a 2:1 ratio of adult virgin *elav-GAL4* females to adult UAS-HA-V5-LaccID males. Wandering L3 larvae were dissected in cold PBS and fixed in 4% PFA for 20 min. Following fixation, L3 filets were washed in PTX (PBS and 0.02% Triton X-100) and blocked in PBT (PBS, 0.02% Triton X-100 and 1% NGS) on a nutator and incubated with primary antibodies for either 2 h at room temperature or overnight at 4 °C with agitation. The following primary antibodies were used: mouse anti-V5 (1:100; R960-25, Thermo Fisher) and rat anti-Elav (1:100; Developmental Studies Hybridoma Bank). The following species-specific secondary antibodies were used: AlexaFluor 488 at 1:300 and AlexaFluor 594-conjugated anti-HRP (Jackson Immunoresearch Laboratories; used to label motor neuron membranes) at 1:300.

Following immunostaining, L3 central nervous system (CNS) or body walls were mounted in SlowFade Gold (Invitorgen) and fluorescent images were acquired on a LSM 980 (Carl Zeiss) using a \times 20 objective (for the CNS) or \times 40/ \times 63 objective (for the NMJ).

Preparation of Ce-DAB2-stained fly tissues for EM

Fly brains and spinal cords were dissected according to previously described methods. In brief, brains and spinal cords were rapidly dissected in cold 0.15 M sodium cacodylate pH 7.4 containing 4% paraformaldehyde (PFA) and 0.5% glutaraldehyde. After dissection, tissues were fixed for 2–3 h in the same fixative on ice. Tissues were then put into 0.15 M sodium cacodylate pH 7.4 containing 2.5% glutaraldehyde and fixed for additional 20 min at 4 °C. Unreacted glutaraldehyde was quenched by incubating the tissues in 50 mM glycine in 0.15 M cacodylate buffer for 20 min at 4 °C. After quenching, tissues were gently washed five times with 0.15 M cacodylate buffer.

Ce-DAB2 staining and preparation of $\it Drosophila$ larval CNS for EM

The dissected flies' central brain and VNC were rinsed (five times for 3 min each) with 0.15 M sodium cacodylate buffer pH 7.4 containing 2 mM CaCl₂ on ice and blocked with 20 mM glycine, 50 mM potassium

cyanide and 50 mM aminotriazole in 0.15 M sodium cacodylate buffer pH7.4 containing 2 mM CaCl_2 for 20 min on ice. Flies were then washed (twice for 1 min each) with 0.15 M sodium cacodylate buffer pH 7.4 containing 2 mM CaCl_2 on ice and were reacted with 2.5 mM Ce-DAB2 solution in cacodylate buffer 36 for 75 min to produce the desired brown intensity color from the precipitate. Flies were washed (five times for 3 min each) with 0.15 M sodium cacodylate buffer pH 7.4 containing 2 mM CaCl_2 on ice, postfixed with 1% osmium tetroxide in 0.15 M sodium cacodylate buffer pH 7.4 for 1 h on ice, washed (five times for 3 min each) with ddH20 on ice and dehydrated in an ethanol series (20%, 50%, 70%, 90% and 100%) for 5 min each on ice, then 100% dry ethanol at room temperature twice for 5 min each, then 1:1 v/v dry ethanol and dry acetone for 5 min at room temperature.

Flies were infiltrated with 25% Durcupan epoxy resin to 75% dry acetone for 4 h, 50% Durcupan epoxy resin to 50% dry acetone overnight, 75% Durcupan epoxy resin to 25% dry acetone for 8 h, 90% Durcupan epoxy resin to 10% dry acetone overnight and Durcupan ACM (four times for 8-12 h each) and then embedded in a vacuum oven at 60 °C for 1 week.

TEM

First, 100-nm-thick sections were cut by an Ultra 45° Diatome diamond knife using a Leica Ultracut UCT ultramicrotome. Both laccase-positive and laccase-negative flies were cut in the coronal plane from dorsal to ventral. Sections were picked up on a 50-mesh copper grid (Ted Pella, G50) and were carbon-coated on both sides by a Cressington 208 carbon coater to prevent charging of the plastic, which can cause drift and thermal damage.

TEM images of laccase in plasma membranes in both cultured cells and flies were acquired with a FEI Spirit at 80 kV. Fly images were taken posterior and lateral from median line regions adjacent to VNC.

EELS and EFTEM

Both electron energy loss spectroscopy (EELS) and energy-filtered TEM (EFTEM) were performed with an in-column Omega filter JEOL JEM-3200EF TEM operating at 300 kV with a LaB6 electron source. The samples were preirradiated for about 30 min at a low magnification to stabilize the sample and minimize contamination. The electron energy loss spectrum, zero-loss images and energy-filtered elemental maps were acquired using an Ultrascan 4000 charge-coupled detector from Gatan. The EELS acquisition was 60 s long using a 4,000 × 4,000 pixel format with a 180-eV slit. The cerium elemental map was obtained at the M5,4 core-loss edge, the onset of which occurs at 883 eV. The EFTEM images before and after edges were obtained using a slit width of 35 eV and 20 datasets were collected for each window before and after the edge at 815 eV, 855 eV and 899 eV. For each window, 20 images were corrected for X-rays, aligned, stacked and sum-stacked by z projection using Fiji software. Power-law background subtraction was used to create elemental maps of cerium. The elemental map merge and overlay on the TEM image was accomplished as previously reported.

Primary human T cell isolation and culture

Human T cells were isolated and cultured as previously described 52 . In brief, primary CD8 $^+$ T cells were isolated from the blood of anonymous donors (Stanford Blood Center) by negative selection (StemCell Technologies, 17953). T cells were cultured in human T cell medium (HTCM) consisting of X-Vivo 15 (Lonza, 04-418Q), 5% human AB serum (Fisher Scientific, NC9310328) and 10 mM neutralized *N*-acetyl-L-cysteine (Sigma-Aldrich, A9165) supplemented with 30 U per ml IL-2 (PeproTech, 200-02 or BRB preclinical biologics repository, National Institutes of Health (NIH)) at 37 $^{\circ}$ C under 5% CO₂.

Engineering of primary human T cells and in vitro killing assay Engineered TCR and CAR receptors recognize the NY-ESO-1₁₅₇₋₁₆₅ pep

Engineered TCR and CAR receptors recognize the NY-ESO- $1_{157-165}$ peptide presented by HLA-A*02:01. The engineered TCR used for this

experiments, 1G4, is an enhanced affinity TCR previously reported 53 . The engineered CAR used the scFv regions previously described 42,54 but with the CD8a hinge/TM domains and 4-1BB costimulatory domain. Both engineered receptors had a C-terminal MYC tag to allow detection of receptor surface expression by flow cytometry.

Lentivirus was produced by transfecting HEK293T cells plated in a T75 flask with 6 μg of psPAX2, 3 μg of pMD2.G and 12 μg of lentiviral vector containing the LaccID, TCR or CAR with 60 μl of PEI Max (1 mg ml $^{-1}$ in water, pH 7.3). Lentivirus was collected at 24 and 48 h after transfection and filtered through a 0.22- μm or 0.45- μm filter. Then, 30 ml of lentivirus supernatant was concentrated by centrifugation at 20,000g at 4 °C for 2 h and then resuspended in 600 μl of StemMACS HSC expansion medium (Miltenyi Biotec). The concentrated lentivirus was used immediately or stored at -80 °C.

Isolated T cells were activated with human T activator CD3/CD28 Dynabeads (Life Technologies, 11131D) at a 1:1 cell-to-bead ratio for 24 h before transduction. Activated T cells were transduced with concentrated virus in StemMACS and HTCM supplemented with IL-2 was replenished at 24 h after transduction and every other day. Expression of LaccID and engineered receptors was verified at 96 h after transduction by flow cytometry (day 5). Cells coexpressing LaccID and the engineered receptor were sorted, expanded and maintained at a cell density of 0.5–1 million cells per ml until day 14.

Sample preparation for T cell proteomics

A375 melanoma tumor cells (ATCC, CRL-1619) were cultured in complete DMEM (Gibco, 11965-092) supplemented with 10% (v/v) FBS (VWR, 97068-085) and 1% penicillin-streptomycin (VWR, 16777-164) at 37 °C under 5% CO₂. A total of 4 million A375 cells were seeded in a 150-mm dish and, 24 h later, when the tumor cell population reached approximately 10 million, 30 million CD8+ primary human T cells expressing LaccID and a constitutive engineered receptor (TCR or CAR) or T cells expressing only LaccID (no TCR or CAR) were added to the culture, achieving an effector to target ratio of 3:1. The T cells and A375 tumor targets were cocultured at 37 °C with 5% CO₂ for 24 h. Subsequently, the cells were labeled with 250 µM BMP for 2 h and then quenched with quenchers (10 mM sodium ascorbate and 5 mM Trolox). The 40 million cells were pelleted and washed three times with DPBS containing quenchers. The cells were lysed in 1 ml of RIPA lysis buffer (Millipore) containing protease inhibitor cocktail, radical quenchers, 10 mM sodium azide and benzonase, Next, 50 ul of the lysate was reserved for western blotting and the remainder was used for streptavidin enrichment following the protocol described previously⁷. Streptavidin beads were washed twice with 1 ml of RIPA buffer and incubated with the cell lysate for 1 hat room temperature with rotation. The beads were then washed three times with 1 ml of RIPA buffer, followed by washes with 1 M KCl, 0.1 M Na₂CO₂ and 2 M urea in 10 mM Tris-HCl (pH 8.0). The beads were then washed with 1 ml of RIPA two more times. Finally, the beads were washed twice with 75 mM NaCl in 50 mM Tris-HCl (pH 8.0), frozen in 50 µl of the buffer and stored until further processing.

On-bead trypsin digestion of biotinylated proteins

Biotinylated proteins bound to streptavidin magnetic beads were subjected to four washes with 200 μ l of 50 mM Tris-HCl (pH7.5) buffer. After removing the final wash, the beads were incubated twice at room temperature in 80 μ l of the digestion buffer (2 M urea, 50 mM Tris-HCl, 1 mM DTT and 0.4 μ g of trypsin) while shaking at 1,000 rpm. The first incubation lasted 1 h, followed by the second incubation of 30 min. After each incubation, the supernatant was collected and transferred into a separate tube. The beads were then washed twice with 60 μ l of 2 M urea in 50 mM Tris-HCl buffer. The resulting washes were combined with the digestion supernatant. The pooled eluate of each sample was then spun down at 5,000g for 30 s to collect the supernatant. The samples were subsequently reduced with 4 mM DTT for 30 min at

room temperature with shaking at 1,000 rpm, followed by alkylation with 10 mM iodoacetamide for 45 min in the dark at room temperature while shaking at 1,000 rpm. Overnight digestion of the samples was performed by adding 0.5 μ g of trypsin to each sample. The following morning, the samples were acidified with neat formic acid to the final concentration of 1% formic acid (pH < 3.0).

Digested peptide samples were desalted using in-house packed C18 (3M) StageTips. C18 StageTips were conditioned sequentially with $100~\mu l$ of 100% methanol, $100~\mu l$ of 50% (v/v) acetonitrile with 0.1% (v/v) formic acid and two washes of $100~\mu l$ of 0.1% (v/v) formic acid. Acidified peptides were loaded onto the C18 StageTips and washed twice with $100~\mu l$ of 0.1% formic acid. The peptides were then eluted from the C18 resin using $50~\mu l$ of 50% acetonitrile with 0.1% formic acid. The desalted peptide samples were snap-frozen and vacuum-centrifuged until completely dry.

TMT labeling and fractionation

Desalted peptides were labeled with TMTpro reagents (Thermo Fisher Scientific). Each peptide sample was resuspended in 80 μ l of 50 mM HEPES and labeled with 20 μ l of the 25 μ g μ l $^{-1}$ TMT reagents in acetonitrile. The samples were then incubated at room temperature for 1 h while shaking at 1,000 rpm. To quench the TMT-labeling reaction, 4 μ l of 5% hydroxylamine was added to each sample, followed by a 15-min incubation at room temperature with shaking. TMT-labeled samples were combined and vacuum-centrifuged to dry. The samples were then reconstituted in 200 μ l of 0.1% formic acid and desalted on a C18 StageTips using the previously described protocol. The desalted TMT-labeled combined sample was then dried to completion.

The combined TMT-labeled peptide sample was fractionated by basic reverse phase (bRP) fractionation using an in-house packed SDB-RPS (3M) StageTip. The SDB-RPS StageTip was first conditioned sequentially with $100~\mu l$ of 100% methanol, $100~\mu l$ 50% acetonitrile with 0.1% formic acid and two washes of $100~\mu l$ of 0.1% formic acid. The peptide sample was reconstituted in 0.1% formic acid and loaded onto the SDB-RPS StageTip. Peptides were then eluted from the StageTip in eight fractions using 20 mM ammonium formate buffers with increasing (v/v) concentrations of acetonitrile (5%, 7.5%, 10%, 12.5%, 15%, 20%, 25% and 45%). The eight fractions were then dried down to completion.

Liquid chromatography-mass spectrometry

All peptide samples were separated and analyzed on an online liquid chromatography-tandem mass spectrometry (LC-MS/MS) system, consisting of a Vanquish Neo ultrahigh-performance LC (Thermo Fisher Scientific) coupled to an Orbitrap Exploris 480 (Thermo Fisher Scientific). All peptide fractions were reconstituted in 9 µl of 3% acetonitrile with 0.1% formic acid. Then, 4 µl of each fraction was injected onto a microcapillary column (Picofrit with 10-µm tip opening and 75-μm diameter; New Objective, PF360-75-10-N-5), packed in-house with 30 cm of C18 silica material (1.5 μm of ReproSil-Pur C18-AQ medium; Dr. Maisch, r119.aq) and heated to 50 °C using column heater sleeves (PhoenixST). Peptides were eluted into the Orbitrap Exploris 480 at a flow rate of 200 nl min⁻¹. The bRP fractions were run on for 110 min, including a linear 84-min gradient from 94.6% solvent A (0.1% formic acid) to 27% solvent B (99.9% acetonitrile, 0.1% formic acid), followed by a linear 9-min gradient from 27% solvent B to 54% solvent B.

MS was conducted using a data-dependent acquisition mode, where MS1 spectra were measured with a resolution of 60,000, a normalized automatic gain control target of 300% and a mass range from 350 to 1,800 m/z. MS2 spectra were acquired for the top 20 most abundant ions per cycle at a resolution of 45,000, an AGC target of 30%, an isolation window of 0.7 m/z and a normalized collision energy of 34. The dynamic exclusion time was set to 20 s and the peptide match and isotope exclusion functions were enabled.

Analysis of MS data

MS data were processed using Spectrum Mill (proteomics.broadinstitute.org). Spectra within a precursor mass range of 600-6,000 Da with a minimum MS1 signal-to-noise ratio of 25 were retained. Additionally, MS1 spectra within a retention time range of ± 45 s or within a precursor m/z tolerance of $\pm 1.4 \, m/z$ were merged. MS/MS searching was performed against the human UniProt database (released on September 2,2021), supplemented with the sequence of LaccID to track its expression across samples. For searching, the full-mix function of the TMTpro modification with the fixed modification of carbamidomethylation on cysteine was used. Variable modifications included acetylation of the protein N terminus, oxidation of methionine, cyclization to pyroglutamic acid and N-terminal deamidation. Digestion parameters were set to 'trypsin allow P' with an allowance of four missed cleavages. The matching tolerances were set with a minimum matched peak intensity of 30%, precursor and product mass tolerance of ±20 ppm and a maximum ambiguous precursor charge of 3.

Peptide spectrum matches (PSMs) were validated with a maximum FDR threshold of 1.2% for precursor charges ranging from \pm 2 to \pm 6. A target protein score of 0 was applied during protein polishing autovalidation to further filter PSMs. TMTpro reporter ion intensities were corrected for isotopic impurities using the afRICA correction method in the Spectrum Mill protein/peptide summary module, which uses determinant calculations according to Cramer's rule. Protein quantification and statistical analysis were performed using the Proteomics Toolset for Integrative Data Analysis (Protigy, version 1.0.7, Broad Institute; https://github.com/broadinstitute/protigy). Differential protein expression was evaluated using moderated t-tests, with t-t-values calculated to assess significance.

Surface proteomic data analysis

To generate monoculture and coculture surfaceomes, a percent sequence coverage filter was applied with a 4% cutoff as it improved specificity of the datasets. Then, the filtered datasets were compared to the Omit LaccID condition, using a P-value cutoff of 0.01 and an FDR of 5% for monocultures and 10% for cocultures (Supplementary Table 2 and Supplementary Figs. 9f and 10b). The FDR was calculated using a subset of false-positive proteins expected not to be labeled by LaccID: nucleus and cytosol proteins that were not annotated with terms related to the cell surface, Golgi or membrane (Supplementary Table 4). The cell surface annotation rate was calculated using a subset of proteins expected to be exposed on the cell surface, which are annotated in UniProt⁵⁵, Human Protein Atlas⁵⁶ and Gene Ontology (GO) cellular $component {}^{57,58}\, terms\, including\, cell\, membrane,\, cell\, surface,\, secreted$ (secretory granule, synaptic vesicle), endosomes (early, late, recycling, membrane), lysosome, plasma membrane (basal, apical, lateral, external side, raft), extracellular regions (space, matrix, vesicle, exosome), immunological synapse, cilium, intercellular bridge, membrane raft, junctions (adherens, bicellular tight, anchoring, cell-cell), presynaptic membrane, early endosome, basement membrane, exocyst, ruffle membrane and focal adhesion (Supplementary Table 4). Golgi and ER proteins used in Fig. 5c are listed in Supplementary Table 4.

To compare cocultures versus monocultures, filtered datasets of each were combined and filtered using a P-value cutoff of 0.01. Proteins were then ranked by \log_2 fold change (coculture over monoculture). The GO cellular component and biological process of top 50 proteins and bottom 40 proteins were analyzed by g:Profiler 59 .

Reporting summary

Further information on research design is available in the Nature Portfolio Reporting Summary linked to this article.

Data availability

The data associated with this study are available in the article and the Supplementary Information. Mass spectrometry protemoics data

are available from ProteomeXchange through the PRIDE database under accession code PXD062870 and MassIVE under accession code MSV000095684. MS/MS searching was performed against the human UniProt database (released on 2 September 2021). Source data are provided with this paper.

References

- Hernandez-Lopez, R. A. et al. T cell circuits that sense antigen density with an ultrasensitive threshold. Science 371, 1166–1171 (2021).
- Robbins, P. F. et al. Single and dual amino acid substitutions in TCR CDRs can enhance antigen-specific t cell functions. J. Immunol. 180, 6116–6131 (2008).
- Maus, M. V. et al. An MHC-restricted antibody-based chimeric antigen receptor requires TCR-like affinity to maintain antigen specificity. *Mol. Ther. Oncolytics* 3, 1–9 (2016).
- 55. Consortium, T. U. UniProt: the Universal Protein Knowledgebase in 2023. *Nucleic Acids Res.* **51**, D523–D531 (2022).
- 56. Thul, P. J. et al. A subcellular map of the human proteome. *Science* **356**, eaal3321 (2017).
- 57. Ashburner, M. et al. Gene Ontology: tool for the unification of biology. *Nat. Genet.* **25**, 25–29 (2000).
- The Gene Ontology Consortiumet al. The Gene Ontology knowledgebase in 2023. Genetics 224, iyad031 (2023).
- Kolberg, L. et al. g:Profiler—interoperable web service for functional enrichment analysis and gene identifier mapping (2023 update). *Nucleic Acids Res.* 51, W207–W212 (2023).

Acknowledgements

We thank M. Sanchez (University of Cambridge) for initial assistance with directed evolution. We also thank P. Tao and Q. Xue (Stanford University) for protocols and reagents related to T cell flow cytometry. This work was supported by the NIH (RC2DK129964 to A.Y.T., RO1-DC006982 to L.L. and K99-DC021195 to C.N.M.), National Science Foundation (NeuroNex UTA20-000889 to A.Y.T. and 2014862 to M.H.E), Wu Tsai Neurosciences Institute (Phil & Penny Knight Initiative for Brain Resilience to A.Y.T. and Neuro-omics grant to A.Y.T. and L.L.), grant I+D+I PID2022-142074OBI00-RAINBOW funded by MCIN/ AEI/10.13039/501100011033/FEDER, UE (to M.A.), Comunidad de Madrid Atraccion de Talento Mod. 1 Project 2022-T1/BIO-23851/ECOCHEM. (to D.G.P.), the Swiss National Science Foundation Postdoc Mobility

fellowship (to D.H.) and the DGIST Start-up Fund Program of the Ministry of Science (ICT 2025020055 to S.-Y.L.). This work was also supported in part by a grant from the Dr. Miriam and Sheldon G. Adelson Medical Research Foundation to N.D.U. and S.A.C. R.A.H.-L. holds a Career Award at the Scientific Interface from Burroughs Welcome Fund. A.Y.T. and R.A.H.-L. are Chan Zuckerberg Biohub San Francisco investigators.

Author contributions

A.Y.T. and S.-Y.L. conceived of the project. S.-Y.L., H.R. and A.Y.T. designed the experiments and analyzed all the data except where noted. S.-Y.L. and H.R. performed all the experiments, unless otherwise noted. M.A. and D.G.P. provided the laccase variants, generated the recombinant laccases and performed the in vitro characterization of LaccID and LacAnc100. M.H.E., M.R.M., S.R.A. and K.-Y.K., generated the EM samples, performed the EM imaging and analyzed the EM images. R.H.L., D.H. and S.-Y.L. isolated and cultured the human primary T cells. S.A.C., N.D.U. and K.N. performed the post-streptavidin-enrichment sample processing, MS and initial data analysis. L.L., C.N.M. and D.J.L. produced and characterized the transgenic flies for EM imaging. C.L. tested for the surface expression of intracellular proteins. A.Y.T., S.-Y.L. and H.R. wrote the paper with input from all authors.

Competing interests

A.Y.T. is a scientific advisor to Third Rock Ventures and Nereid Therapeutics. The remaining authors declare no competing interests.

Additional information

Supplementary information The online version contains supplementary material available at https://doi.org/10.1038/s41589-025-01973-6.

Correspondence and requests for materials should be addressed to Alice Y. Ting.

Peer review information *Nature Chemical Biology* thanks Rudi Fasan and the other, anonymous reviewer(s) for their contribution to the peer review of this work.

Reprints and permissions information is available at www.nature.com/reprints.

nature portfolio

Corresponding author(s):	Alice Y. Ting
Last updated by author(s):	Mar 10, 2025

Reporting Summary

Nature Portfolio wishes to improve the reproducibility of the work that we publish. This form provides structure for consistency and transparency in reporting. For further information on Nature Portfolio policies, see our <u>Editorial Policies</u> and the <u>Editorial Policy Checklist</u>.

~				
5	רם:	tic	:†ı	CC

For a	ll statistical analyses, confirm that the following items are present in the figure legend, table legend, main text, or Methods section.
n/a	Confirmed
	\boxtimes The exact sample size (n) for each experimental group/condition, given as a discrete number and unit of measurement
	🔀 A statement on whether measurements were taken from distinct samples or whether the same sample was measured repeatedly
	The statistical test(s) used AND whether they are one- or two-sided Only common tests should be described solely by name; describe more complex techniques in the Methods section.
	A description of all covariates tested
\boxtimes	A description of any assumptions or corrections, such as tests of normality and adjustment for multiple comparisons
	A full description of the statistical parameters including central tendency (e.g. means) or other basic estimates (e.g. regression coefficient) AND variation (e.g. standard deviation) or associated estimates of uncertainty (e.g. confidence intervals)
	For null hypothesis testing, the test statistic (e.g. <i>F</i> , <i>t</i> , <i>r</i>) with confidence intervals, effect sizes, degrees of freedom and <i>P</i> value noted Give P values as exact values whenever suitable.
	For Bayesian analysis, information on the choice of priors and Markov chain Monte Carlo settings
	For hierarchical and complex designs, identification of the appropriate level for tests and full reporting of outcomes
	Estimates of effect sizes (e.g. Cohen's d , Pearson's r), indicating how they were calculated
'	Our web collection on statistics for biologists contains articles on many of the points above.
Sof	tware and code
Policy	information about <u>availability of computer code</u>
Dat	Odvssey DLy Imaging System ChemiDoc Imaging Systems Slidehook 6.0. RD EACSDiva 8.0.1. Righted Everest

Data

Data analysis

Policy information about availability of data

All manuscripts must include a data availability statement. This statement should provide the following information, where applicable:

Slidebook 6.0, ImageJ 1.53k,, Image Studio v5.5.4, Spectrum Mill v7.11, FlowJo v10, Protigy v1.0.7, Snapgene v6

For manuscripts utilizing custom algorithms or software that are central to the research but not yet described in published literature, software must be made available to editors and reviewers. We strongly encourage code deposition in a community repository (e.g. GitHub). See the Nature Portfolio guidelines for submitting code & software for further information.

- Accession codes, unique identifiers, or web links for publicly available datasets
- A description of any restrictions on data availability
- For clinical datasets or third party data, please ensure that the statement adheres to our policy

The data associated with this study are available in the article and the Supplementary Information. The original mass spectra and the protein sequence database used for searches have been deposited in the public proteomics repository MassIVE (http://massive.ucsd.edu) and are accessible at ftp:// MSV000095684@massive.ucsd.edu. MS/MS searching was performed against a human Uniprot database, released on September 02, 2021

Human rese	arch part	icipants		
Policy information	about <u>studies</u>	involving human research participants and Sex and Gender in Research.		
Reporting on sex and gender		N/A		
Population chara	acteristics	N/A		
Recruitment		N/A		
Ethics oversight		N/A		
Note that full informa	ation on the app	roval of the study protocol must also be provided in the manuscript.		
Field-spe	ecific re	eporting		
Please select the o	ne below that	is the best fit for your research. If you are not sure, read the appropriate sections before making your selection.		
X Life sciences		Behavioural & social sciences		
For a reference copy of	the document with	n all sections, see <u>nature.com/documents/nr-reporting-summary-flat.pdf</u>		
Life scier	nces st	udy design		
All studies must dis	sclose on these	e points even when the disclosure is negative.		
Sample size	Biotechnology by a spectroph For samples fo in all phases o For mammalia	st library sortings, we prepared minimum 10x library size of cells, consistent with published yeast display evolution of TurboID (Nature inology, Vol 36, 880-887 (2018)). We assumed optical density (OD600) of 1.0 corresponds to 1 x 10e7 cells / mL. OD600 was measured ectrophotometer. The ples for mass spectrometry, triplicate biological replicates for experimental samples and duplicate for control samples were evaluated hases of our study, which is acceptable for proteomics studies in biological systems. The management of the proteomics of the management of the proteomics of the		
Data exclusions	No data were	a were excluded from analyses.		
Replication	Two to three i	Two to three independent replicates were performed by different hands. We confirmed all results were reproducible.		
Randomization	Randomization	n was not relevant for this study since the measurement outcome cannot be affected by bias.		
Blinding	The operators were not blinded. The data was collected and analyzed in an objective manner without any bias.			
 		pecific materials, systems and methods s about some types of materials, experimental systems and methods used in many studies. Here, indicate whether each material,		
system or method lis	ted is relevant to	o your study. If you are not sure if a list item applies to your research, read the appropriate section before selecting a response.		
Materials & ex	perimental :	systems Methods		
n/a Involved in the study		n/a Involved in the study		
Antibodies Fulcaryatic call lines		ChIP-seq		
Eukaryotic cell lines Palaeontology and archaeology		□ S Flow cytometry Dlogy MRI-based neuroimaging		

Antibodies

Antibodies used

 ${\color{red} igwedge}$ Animals and other organisms

Dual use research of concern

Clinical data

Antibody, vendor, catalog number: Anti-V5, Thermo Fischer Scientific, R96025; Anti-myc, Exalpha Biologicals, Inc., ACMYC; Streptavidin-PE, Jackson ImmunoResearch, 0.16110084; Anti-Calreticulin, Thermo Fisher Scientific, PA3900; Anti-N-Cadherin, Thermo

Scientific, PA5-19486; Anti-HRP-AlexaFluor594, Jackson Immunoresearch Laboratoris Inc, 123-585-021; Anti-elav, Developmental Studies Hybridoma Bank, 7E8A10; Anti-HSPA9, abcam, ab2799; Anti-PHB1, GeneTex, GTX101105; Anti-OAT, GeneTex, GTX637995; Anti-SHMT2, Cell Signaling Technology, 93566; Anti-ETFB, abcam, ab73986; Anti-CD69, Invitrogen, 17-0699-42; Anti-mouse-AlexaFluor488, Invitrogen, A11001; Anti-chicken-AlexaFluor488, Invitrogen, A11039; Anti-rabbit-AlexaFluor568, Invitrogen, A11011; Anti-chicken-AlexaFluor647, Invitrogen, A21449; Anti-mouse-IRDye 800CW, LI-COR Biosciences, 92632210; Anti-mouse-IRDye 680CW, LI-COR Biosciences, 92632211; Anti-rabbit-IRDye 680CW, LI-COR Biosciences, 92668071; Anti-mouse-HRP, BioRad, 1706515; Anti-rabbit-HRP, BioRad, 1706515; Anti-V5-iFluor488, Genscript, A01803-100

Validation

Anti-V5: https://www.thermofisher.com/antibody/product/V5-Tag-Antibody-clone-SV5-Pk1-Monoclonal/R960-25 Anti-myc: Anti-myc: https://www.exalpha.com/products/chicken-anti-c-myc-epitope-tag/ACMYC4 Anti-Calreticulin: https://www.thermofisher.com/antibody/product/Calreticulin-Antibody-Polyclonal/PA3-900 Anti-N-Cadherin: https://www.thermofisher.com/antibody/product/N-cadherin-Antibody-Polyclonal/PA5-19486 Anti-elav: https://dshb.biology.uiowa.edu/Rat-Elav-7E8A10-anti-elav
Anti-V5-iFluor488: https://www.genscript.com/antibody/A01803-THE_V5_Tag_Antibody_iFluor_488_mAb_Mouse anti-HSPA9: https://www.abcam.com/en-us/products/primary-antibodies/grp75-mot-antibody-jg1-ab2799 anti-PHB1: https://www.genetex.com/Product/Detail/Prohibitin-antibody/GTX101105 anti-OAT: https://www.genetex.com/Product/Detail/OAT-antibody-HL2087/GTX637995 anti-SHMT2: https://www.cellsignal.com/products/primary-antibodies/shmt2-e7x5b-rabbit-mab/93566

anti-ETFB: https://www.abcam.com/en-us/products/primary-antibodies/etfb-antibody-ab73986
Anti-CD69-APC: https://www.thermofisher.com/antibody/product/CD69-Antibody-clone-FN50-Monoclonal/17-0699-42

Eukaryotic cell lines

Policy information about <u>cell lines and Sex and Gender in Research</u>

Cell line source(s)

- HEK293T, K562, and A375 cells from ATCC
- Primary CD8+ T cells isolated from blood of anonymous donors (Stanford Blood Center)

Authentication Not authenticated

Mycoplasma contamination The cells were not tested for mycoplasma contamination

Commonly misidentified lines (See ICLAC register)

No misidentified lines were used

Animals and other research organisms

Policy information about <u>studies involving animals</u>; <u>ARRIVE guidelines</u> recommended for reporting animal research, and <u>Sex and Gender in Research</u>

Laboratory animals

Drosophila melanogaster, Wandering third instar larvae (L3)

Wild animals

no wild animals were used in the study

Reporting on sex

N/A

Field-collected samples

no field collected samples were used in the study

Ethics oversight

the study didn't require an ethical approval

Note that full information on the approval of the study protocol must also be provided in the manuscript.

Flow Cytometry

Plots

Confirm that:

The axis labels state the marker and fluorochrome used (e.g. CD4-FITC).

The axis scales are clearly visible. Include numbers along axes only for bottom left plot of group (a 'group' is an analysis of identical markers).

All plots are contour plots with outliers or pseudocolor plots.

A numerical value for number of cells or percentage (with statistics) is provided.

Methodology

Sample preparation

EBY100 yeast cells were cultured and prepared as following a previously published yeast display based directed evolution protocol (Nature Biotechnology, Vol 15, 553-557 (1997)).

Instrument BD Aria II cell sorter (BD Biosciences)

Software BD Biosciences-US and FlowJo

Cell population abundance Top 0.1~0.2% cells were collected. Activity was tested by comparing BP labeling activity of the enriched population to that of previous population.

Gating strategy

To sort on a BD FACS Aria II cell sorter (BD Biosciences), gates for singlets were drawn on an FSC-A by SSC-A plot to generate

population 1 (P1). This population was then gated on an FSC-A by FSC-H plot to generate population 2 (P2), and then by SSC-A by SSC-W plot to further filter for singlets to generate population 3 (P3). P3 was then gated with rectangular gates drawn for positive selection of high expression and high activity on the top right corner of the Anti-myc-AF488 (or AF647) by SA-PE signal plot to coolect the top ~0.1-0.2%.

Tick this box to confirm that a figure exemplifying the gating strategy is provided in the Supplementary Information.